Dual roles of inorganic aqueous phase on SOA growth from benzene and phenol

Jiwon Choi[1], Myoseon Jang[1,*], and Spencer Blau[1]

[1]Department of Environmental Engineering Sciences, University of Florida, Gainesville, 32611, USA

5 *Correspondence to*: Myoseon Jang (mjang@ufl.edu)

Abstract. Benzene, emitted from automobile exhaust and biomass burning, is ubiquitous in ambient air. Benzene is a precursor hydrocarbon (HC) that forms secondary organic aerosols (SOA), but its SOA formation mechanism is not well studied. To accurately predict the formation of benzene SOA, it is important to understand the gas mechanisms of phenol, which is one of the major products formed from the atmospheric oxidation of benzene. ~~Our chamber study found that wet~~ 10 ~~inorganic aerosol retarded the gas oxidation of phenol or benzene, and thus their SOA formation.~~ Laboratory data presented herein highlights the impact of aqueous phase on SOA generated through benzene and phenol oxidation. The roles of the aqueous phase consist in: (1) suppression in aging of hydrocarbon and (2) conventional acid-catalyzed reaction in inorganic phased. To explain this unusual effect, it is hypothesized that a persistent phenoxy radical (PPR) effectively forms via a heterogeneous reaction of phenol and phenol-related products in the presence of wet-inorganic aerosol. These PPR species 15 are capable of catalytically consuming ozone during a NO_x cycle and negatively influencing SOA growth. In this study, explicit gas mechanisms were derived to produce the oxygenated products from the atmospheric oxidation of phenol or benzene. Gas mechanisms include the existing Master Chemical Mechanism (MCM v3.3.1); the reaction path for peroxy radical adducts originating from the addition of an OH radical to phenols forming low-volatility products (e.g., multi-hydroxy aromatics); and the mechanisms to form heterogeneous production of PPR. The simulated gas products were 20 classified into volatility-reactivity based lumping species and incorporated into the UNIfied Partitioning Aerosol Reaction (UNIPAR) model that predicts SOA formation via multiphase reactions of phenol or benzene. The predictability of the UNIPAR model was examined using chamber data, which were generated for the photooxidation of phenol or benzene under controlled experimental conditions (NO_x levels, humidity, and inorganic seed types). The SOA formation from both phenol and benzene still increased in the presence of wet inorganic seed because of the oligomerization of reactive organic species 25 in aqueous phase. However, model simulations show a significant suppression in ozone, the oxidation of phenol or benzene, and SOA growth, compared to those without PPR mechanisms. The production of PPR is accelerated in the presence of acidic aerosol and this weakens SOA growth. In benzene oxidation, up to 53% of the oxidation pathway is connected to phenol formation in the reported gas mechanism. Thus, the contribution of PPR to gas mechanisms is less than phenol. Overall, SOA growth in phenol or benzene is negatively related to NO_x levels in the high NO_x region (HC ppbC/NO_x ppb 30 <5). However, the simulation indicates that the significance of PPR rises with decreasing NO_x levels. Hence, the influence of NO_x levels on the SOA formation from phenol or benzene is complex under varying temperature and seed types. Adding the

comprehensive reaction of phenolic compounds will improve the prediction of SOA formation form aromatic HCs due to the missing mechanisms in the current air quality model.

1. Introduction

Hydrocarbons (HCs) are emitted from both anthropogenic sources (e.g., fuel combustion, vehicle exhaust, and industrial activities) and biogenic sources from vegetation (Carlton et al., 2010). The photochemical oxidation of these HCs can produce ozone through incorporating with the NO_x cycle. In addition, the formation of semi-volatile or non-volatile oxygenated products through a series of chemical reactions of precursor HCs in the atmospheric environment can yield Secondary Organic Aerosol (SOA). This SOA constitutes a large proportion organic aerosol in the ambient air, ranging from 20% in mid-latitudes to 90% in tropical forested area (Jimenez et al., 2009; Zhang et al., 2007; Kanakidou et al., 2005). Hence, the estimation of SOA formation potential is important to accurately evaluate the impact of atmospheric organic aerosol on health and climate formation.

Benzene, the simplest aromatic HC, is emitted mainly from automobile exhaust, and it can be found in gases from biomass burning. Benzene, a solvent, is also emitted from industrial processes such as chemical synthesis, construction, and pharmaceutical facilities (Verma and Tombe, 2002; Wang et al., 2014). In addition, benzene is known to be emitted from oceans including remote Southern Ocean and the Arctic marginal ice zone (Wohl et al., 2023). The major atmospheric oxidation path of benzene is the reaction with OH radicals. Benzene's oxidation rate (i.e., 1.22×10^{-12} cm^3 molecules^{-1} sec^{-1} at 298 K) (Borrás and Tortajada-Genaro, 2012) is relatively slow, but its SOA yield is high. According to laboratory studies (Ng et al., 2007), benzene's SOA yields can be even greater than high yield aromatic HCs (i.e., toluene) at a given experimental condition. However, the prediction of benzene SOA has not been well studied due to uncertainties in both gas oxidation mechanisms and aerosol phase reactions that form oligomeric species under various environmental conditions.

In benzene oxidation with an OH radical, about 53% of pathways are linked to the formation of phenol and the remains of oxidation paths are connected to ring opening products in the current Master Chemical Mechanism (MCM v3.3.1) (Bloss et al., 2005). In addition, a significant fraction (20%) of oxygenated aromatic, emitted from biomass burning, is phenol (Akherati et al., 2020). of phenol Hence understanding phenol oxidation mechanisms is a key to predicting benzene oxidation and SOA formation. Phenol gas oxidation includes the reaction path for peroxy radical adducts originating from the addition of an OH radical to phenols to form low volatility products (e.g., multi-hydroxy aromatics). Laboratory studies report that gas oxidation of phenol forms low-volatility Highly Oxygenated Organic Molecules (HOM) (Nakao et al., 2011; Ji et al., 2017; Yee et al., 2013). Phenols are highly reactive to the addition of OH radicals into an aromatic ring due to the electron receiving characteristics of phenolic OH group. Phenols effectively produce multi-hydroxybenzenes compared to conventional alkyl-substituted monocyclic aromatic HCs (Hansch et al., 2000).

In addition to gas mechanisms , increased SOA formation via to form the production of HOM, phenol and phenolic products (e.g., catechols and nitrophenols) can yield Persistent Phenoxy Radicals (PPR), which can potentially suppress atmospheric

oxidation capability and SOA growth. Unlike aliphatic alkoxy radicals, which can react with an oxygen molecule to form a hydroperoxyl (HO_2) radical, PPR have no aliphatic hydrogen at the carbon attached to the O-radical~~.~~. A p-π conjugated system can help stabilizing phenoxy radicals. Thus, ~~the lifetime of~~ these phenoxy radicals have a ~~is~~ relatively long lifetime in ambient air and they can catalytically deplete~~s~~ ozone (Tao and Li, 1999).

In a recent modeling study, Choi and Jang (Choi and Jang, 2022) explicitly predicted phenol gas oxidation including the formation of HOM and other multi-hydroxyphenols (Pillar-Little et al., 2015; Choi and Jang, 2022; Yee et al., 2013; Yu et al., 2016). The resulting oxidation products were categorized into volatility-reactivity based lumping species, and integrated into the UNIfied Partitioning Aerosol Reaction (UNIPAR) model, developed by Im and Jang (Im et al., 2014), which simulated SOA formation via multiphase reactions of HCs. Choi and Jang showed the importance of HOM to predict the formation of phenol SOA through the simulation of chamber data using the UNIPAR model (Choi and Jang, 2022). In the absence of wet-inorganic seed aerosol, where RH was kept above ERH to avoid the crystallization of seed, their model successfully simulated SOA formation, but in the presence of wet-inorganic seed, the model failed to predict both gas oxidation (ozone, NOx, and decay of phenol) and SOA formation. In the last two decades, the impact of aerosol acidity on SOA has been studied in numerous laboratories (Jang et al., 2002; Garland et al., 2006; Hallquist et al., 2009; Deng et al., 2021; Surratt et al., 2007a). The reactive oxygenated products, formed from the oxidation of biogenic and aromatic HCs, undergo acid-catalyzed reactions (e.g., hydration, oligomerization, formation of hemiacetal/acetal/trioxane, aldol condensation, and cationic rearrangement) in the presence of acidic inorganic aerosol, and accelerate SOA formation. However, Choi and Jang observed an unexpected impact of aerosol acidity on SOA formation, which suppressed SOA formation more than neutral, wet-ammonium sulfate (AS) seed. Since the wet-inorganic aerosol suppresses gas oxidation (ozone and the decay of phenol), it is unlikely to be associated with the inaccuracy of oligomerization ~~rates~~ of reactive oxygenated species in aqueous phase. This finding is distinct from the typical SOA formation from alkyl-substituted aromatics or biogenic HCs, which are positively correlated to aerosol acidity (Jang et al., 2002; Hallquist et al., 2009).

In this study, we hypothesize based on chamber experiments and complex model data that the production of PPR from the atmospheric oxidation of phenol and its phenolic products (e.g., catechols and nitrophenols) can be modulated via heterogeneous reactions in wet-inorganic aerosol. The increased PPR via heterogeneous oxidation of phenolic compounds in presence of wet-inorganic aerosol catalytically consumes ozone during a NO_x cycle, and ultimately influences SOA formation from both phenol and benzene. The gas mechanism, named the Heterogeneous Phenoxy Radical model (H-PPR model), was derived to improve the prediction of both gas oxidation of phenol and benzene and their SOA formation in presence of aqueous phase. The prediction of phenol oxidation was improved by integrating HOM and H-PPR into explicit gas mechanisms. In a similar matter, the benzene gas oxidation was improved by using updated phenol mechanisms. Ultimately the resulting gas mechanisms of phenol or benzene were, then, applied to the UNIPAR model to predict SOA formation via multiphase reactions of phenol and benzene. The suitability of the UNIPAR model was demonstrated by comparing simulation~~s~~ and chamber data obtained from the photooxidation of phenol a~~nd~~ b~~nd~~enzene under different experimental conditions in a large outdoor photochemical reactor.

Importantly, both phenol and benzene are abundant in biomass burning smoke and they can largely contribute to SOA formation . Phenol, alongside benzene, are major contributors to the formation of SOA during biomass burning, constituting a substantial portion of the SOA mass generated (Majdi et al., 2019). Despite this recognition, however, several unresolved issues persist, such as understanding the gas-phase mechanisms involved and the role of the aqueous phase in SOA formation. The SOA model of this study can augment the evaluation of the impact of NO_x levels on SOA formation during wildfires under the rural set (low NO_x) and the urban set (high NO_x). The wildfire air plume can transport emissions thousands of km away from the wildfire source (Edwards et al., 2006; Wotawa and Trainer, 2000) influencing background atmosphere air quality (Hudson et al., 2004; Schill et al., 2020). For example, in the Europe Mediterranean area, annually biomass burning emission accounted for 19-21% of organic carbon levels in particulate matter at Barcelona, Spain (Reche et al., 2012). Outdoor chamber data of this study and gas mechanisms of phenols can augment better understanding of the impact of biomass burning smoke on the atmospheric oxidation ability of hydrocarbons and SOA formation in the city.

2. Experiment Section

To generate SOA, the University of Florida Atmospheric PHotochemical Outdoor Reactor (UF-APHOR) was used. The reactor consists of a dual Teflon film chamber, each with a volume of 52 m^3 and a surface area of 86 m^2, and exposed to ambient sunlight. SOA is produced by the photooxidation of phenol (Acros Organics, 99%) or benzene (Sigma-Aldrich, ≥99%) under varying NO_x levels and different inorganic seed types (non-seed, sulfuric acid (SA), ammonium hydrogen sulfate (AHS) wet-ammonium sulfate (AS)). Detailed description of chamber experiment procedure have been reported in previous studies (Beardsley and Jang, 2016; Choi and Jang, 2022; Han and Jang, 2022, 2023; Im et al., 2014; Yu et al., 2021b; Zhou et al., 2019). In summary, NO (2% in N_2, Airgas, USA), HCs, non-reactive CCl_4 (Sigma-Aldrich, ≥99.5%), and inorganic seed aerosol were injected into the chamber before sunrise. HCs (phenol or benzene) were vaporized into the chamber using a glass manifold under clean air streams. For seeded SOA experiments, 0.05M SA, AHS, or 0.05M AS aqueous solution was atomized using a nebulizer (LC STAR, PARI, Starnberg, Germany) into the chamber. For dry-AS seeded experiments, the relative humidity (RH) was controlled below efflorescence relative humidity (ERH), and for wet-AS experiments, the RH was maintained above ERH to prevent the crystallization of seed.

A photometric ozone analyzer (Model 106-L, 2B Technologies, MA, USA) and a chemiluminescence NO/NO_x analyzer (Model 405, 2B technologies, MA, USA) were used to monitor the concentrations of NO_x and ozone. The error associated with NO, NO_2, and O_3 are 2%. A Gas Chromatograph with a Flame Ionization Detector (GC-FID) (7820A, Agilent Technologies, CA, USA) was employed to measure the concentrations of phenol or benzene. The Proton Transfer Reaction-Time of Flight (PTR-ToF-MS) (PTR 3C, Kore Technology, Cambridgeshire, UK) was also utilized to monitor the decay of phenol or benzene. To monitor air dilution in the chamber, CCl_4 was introduced into the chamber and measured using GC-FID.

The Scanning Mobility Particle Sizer (SMPS) comprising the aerosol classifier (Model 3082, TSI, MN, USA) and
130   condensation particle counter (Model 3750, TSI) was used to measure the particle population and volume concentration. The
Aerosol Chemical Speciation Monitor (ACSM) was used to measure the quantity of sulfate, ammonium, and nitrate ions in
aerosol phase. An Organic Carbon/Elemental Carbon aerosol analyzer (Sunset Laboratory, OR, USA) was employed to
measure the concentration of organic carbon in the aerosol. The Ion Chromatograph (Compact IC 761) was used to measure
the concentration of water-soluble inorganic species (sulfate, nitrate, and ammonium ions) coupled to a Particle into Liquid
135   Sampler (PILS-IC) (ADISO 2081). All gas data were corrected for chamber air dilution. All aerosol data were corrected for
gas dilution and the aerosol loss to the chamber wall as performed in previous chamber studies (Beardsley and Jang, 2016;
Choi and Jang, 2022; Han and Jang, 2022, 2023; Im et al., 2014; Yu et al., 2021b; Zhou et al., 2019).
A hygrometer (CR1000 measurement and control system, Campbell Scientific, UT, USA) was used to measure temperature
and relative humidity (RH) within the chamber. Sunlight intensity was monitored with a Total UV Radiometer (TUVR,
140   Eppley Laboratory, RI, USA). Table 1 provides a summary of the experimental conditions used in the chamber for this
study. Fig. S1 displays the profiles of sunlight, temperature, and humidity on October 19, 2022.

3. Model Description

3.1 UNIPAR SOA model

The UNIPAR model simulates the SOA formation via multiphase reaction of phenol or benzene. Fig. 1 displays the overall
145   structure of the UNIPAR model. Briefly, the key components of the UNIPAR model are described as follow:

The SOA formation in the model streamlines multiphase partitioning, organic phase (*or*) oligomerization, and aqueous
reactions in an inorganic seeded aqueous phase (*in*).

1~~2~~) As seen in Fig. 1, the oxidized products predicted from near explicit mechanisms of phenol or benzene in gas phase (*g*)
are categorized into 50 lumping groups based on their reactivity and volatility. Table S1 displays the physicochemical
150   parameters (i.e., molecular weight (MW_i), oxygen-to-carbon ratio ($O:C_i$), and hydrogen bonding (HB_i)) of lumping species,
which are used to process multiphase partitioning and aerosol chemistry. The predetermined mathematical equations (Tables
S2-S7) dynamically build the stoichiometric coefficient arrays for each precursor (benzene and phenol). Tables S8 and S9
illustrate major products placed in lumping arrays. No difference appears between Table S8 and Table S9 for the major
product of each lumping group. The estimated stoichiometric coefficient reflects the influence of NO_x levels and gas aging
155   on gas-product distributions. The distribution of products was also influenced by H-PPR as a function of the amount of
sulfuric acid. H-PPR increases the contribution of fresh product distribution.

2~~3~~) The concentration of lumping species is distributed into gas (C_g), organic (C_{or}), and inorganic phases (C_{in}) using
partitioning coefficients estimated based on Pankow's absorptive partitioning model (Pankow, 1994) with vapor pressure,
the estimated activity coefficients of lumping species in both the organic and inorganic phases, and aerosol's average
160   molecular weight in each phase.

34) The resulting C_{or} and C_{in} of each lumping species are applied to process the SOA formation via their multiphase partitioning (OM_P) and aerosol phase reactions (OM_{AR}) in both *or* and *in*.

45) The kinetic parameters to calculate aerosol phase reaction rate constants in *or* and *in*, phases, such as lumping species' reactivity scales and their basicity constants, are reported Section S2. Both organic-phase oligomerization and aqueous reactions of reactive species in inorganic phase yield non-volatile OM in the model.

56) The SOA mass formed from gas-organic partitioning (OM_P) is estimated using the Newtonian method (Schell et al., 2001) based on a mass balance of organic compounds between the gas and particle phases governed by Raoult's law. OM_{AR} is considered to be a pre-existing absorbing material for gas-particle partitioning (Cao and Jang, 2007; Im et al., 2014).

67) The inorganic composition and aerosol acidity, which are predicted using the inorganic thermodynamic model, are incorporated into the UNIPAR model. The deliquescence RH (DRH), which is predicted using the equation derived from the inorganic thermodynamic model and ERH, which is predicted using a pre-trained neural network model based on the inorganic composition (Yu et al., 2021a), are used to determine the aerosol state: wet (organic phase + inorganic aqueous phase) or dry (organic phase + solid-dry inorganic phase).

78) In the model, the formation of dialkylsulfate (Liggio et al., 2005; Surratt et al., 2007b; Li et al., 2015) is simulated by using the Hinshelwood-type reaction (Im et al., 2014). The decreased acidic sulfate due to the dialkylsulfate formation is applied to inorganic compositions to calculate aerosol acidity and aerosol water content for the next step.

3.2 Explicit Gas Mechanisms

The gas oxidation of benzene and phenols was processed with the Master Chemical Mechanism (MCM v3.3.1) (Jenkin et al., 2003) coupled with the reaction path for the formation of HOM products (e.g., multi-hydroxy aromatics) and the mechanisms to form PPR via heterogeneous acid-catalyzed reactions of phenolic compounds. The simulation of the atmospheric oxidation of HCs is performed in a box model platform equipped with the Dynamically Simple Model of Atmospheric Chemical complexity (DSMACC) incorporated with the Kinetic PreProcessor (KPP) (Emmerson and Evans, 2009). The description of the mechanism to form HOM and PPR is shown in the following sections.

3.2.1 HOM Formation

The gas mechanism to form HOM in phenol oxidation has been reported in the recent study by Choi and Jang (2022). Fig. S2 depicts the pathways to form HOM from the oxidation of phenol. The resulting phenol gas mechanisms are integrated with benzene gas oxidation. The oxidation of phenol or benzene begins with the reaction with an OH radical and forms HOM via multigeneration oxidation (Nakao et al., 2011; Yee et al., 2013; Sun et al., 2010; Garmash et al., 2020; Calvert et al., 2002; Atkinson, 2000; Olmez-Hanci and Arslan-Alaton, 2013). HOM includes multi-hydroxy benzenes, phenolic compounds, and the products derived from peroxy radical adducts of multi-hydroxy benzenes. The gas phase reaction rate constant for the addition of the OH radical to different aromatic compounds were calculated using the structure-reactivity relationship using Hammett parameters (Kwok and Atkinson, 1995; Brown and Okamoto, 1958)<s>(Kwok and Atkinson, 1995)</s>

(Brown and Okamoto, 1958)(Brown,JACS, 1958). This estimation method can be reliable when it is used in its database, but extrapolation to organic compounds outside of the database can result in a lack of the assurance of its accuracy.

3.2.2 PPR Formation

The first-generation products from phenol gas oxidation include a phenoxy radical (fraction in oxidation paths: 0.06), catechol (0.657), bicyclic peroxy radical (0.183), and monocyclic peroxy radical (0.1) (Bloss et al., 2005; Jenkin et al., 2003). The resulting phenoxy radical ($C_6H_5O\cdot$) in gas phase can catalytically react with ozone as follows (Tao and Li, 1999),

$$C_6H_5OH + OH \rightarrow C_6H_5O\cdot \tag{R1}$$

$$C_6H_5O\cdot + O_3 \rightarrow C_6H_5OO\cdot \tag{R2}$$

Studies have shown that phenol and benzene have the relatively low minimal incremental reactivity (MIR) or photochemical ozone creation potential (POCP) values (Carter, 1994; Jenkin et al., 2017; Zhang et al., 2021). Such low ozone formation potential can be explained via catalytic consumption of ozone by PPR. Phenyl peroxy radical ($C_6H_5OO\cdot$) is able to regenerate $C_6H_5O\cdot$ via reactions in gas phase with NO, NO_2, and NO_3 reactions (Carter and Atkinson, 1989; Jagiella and Zabel, 2007) as follow:

$$C_6H_5OO\cdot + NO \rightarrow C_6H_5O\cdot + NO_2 \tag{R3}$$

$$C_6H_5OO\cdot + NO_2 \rightarrow C_6H_5O\cdot + NO_3 \tag{R4}$$

$$C_6H_5OO\cdot + NO_3 \rightarrow C_6H_5O\cdot + NO_2 \tag{R5}$$

The catalytic decay of ozone influences the production of the OH radical that can be created via the reaction of water vapor with O(1D), a photolysis product of ozone (Finlayson-Pitts and Pitts, 2000). Furthermore, the oxidation of phenol or coexisting HCs can be retarded due to PPR. Evidently, phenol and benzene are known to have a low incremental reactivity to form ozone (Zhang et al., 2021; Carter, 1994). Fig. 2 illustrates the time series of gas simulations and observations in the UF-APHOR chamber. The gas mechanisms reasonably simulate the low ozone formation and the retarded oxidation of phenol or benzene in the absence of inorganic seed. However, the suppression of gas oxidation capability increased in the presence of wet-AS aerosol and was further amplified with increasing aerosol acidity. This surprising discovery suggests that there should be a reaction path to heterogeneously form PPR.

The formation of phenoxy radicals has been reported in condensed matrixes at low temperatures (Sun et al., 1990), strong liquid acids (Dixon and Murphy, 1976), or gas-phase clusters under specific conditions (Steadman and Syage, 1991). The existence of phenoxy radicals has been detected in strong acidic solutions by using Electron Spin Resonance (ESR) Spectroscopy (Holton and Murphy, 1979). Phenol-like compounds, such as phenol, catechol, and pyrogallol (1,2,3-trihydroxybenzene), partition to salted aqueous aerosol and can heterogeneously react with the aqueous-phase OH radical. Various oxidants such as OH, HO_2, and ozone can partition into aqueous phase, and oxidize hydrophilic organic species. Similar to gas phase, the OH radical can be added into an phenolic aromatic ring to form an OH-added intermediate phenol (HO-C_6H_5·OH) (*phenol_OH_int*) in aqueous phase (Mvula et al., 2001). The resulting *phenol_OH_int* can form the

225 phenoxy radical yielding a water molecule (Das, 2005; Mvula et al., 2001). This reaction step is accelerated by an acid catalysis.

In this study, the H-PPR mechanism was integrated into the explicit gas mechanisms accounting for the impact of aqueous phase on SOA formation from phenol and benzene as illustrated in Fig. 2. In this mechanism, the partitioning of phenols between gas (g) and inorganic (in) phases is kinetically expressed by using the absorption rate constant (k_{on_phenol}) and the

230 desorption rate constant (k_{off_phenol}) as follows.

$$C_6H_5OH(g) \rightarrow C_6H_5OH(in) \qquad k_{on\_phenol} \tag{R6}$$

$$C_6H_5OH(in) \rightarrow C_6H_5OH(g) \qquad k_{off\_phenol} \tag{R7}$$

To describe the production of PPR, phenol is used, but various phenolic compounds can also be involved in the formation of H-PPR. k_{on_phenol} is calculated as follows:

235 $$k_{on\_phenol} = f_{abs} \frac{\omega f_{S\_M}}{4} \tag{Eq.1}$$

f_{S_M} is the aerosol surface area concentration (m^2 m^{-3}): i.e., 4×10^{-3}, m^2 μg^{-1} for the particle size near 100 nm. f_{abs} is the coefficient for the uptake process and set as 2 to gear fast gas-particle partitioning in the model. ω is the mean molecular velocity (m s^{-1}) of each chemical species and is calculated as follows:

$$\omega = \sqrt{\frac{8RT}{\pi MW}} \tag{Eq.2}$$

240 MW is the molecular weight (kg mol^{-1}) of organic species. R is a gas constant (8.314 J mol^{-1} K^{-1}) and T (K) is the an absolute temperature.

In the presence of wet-inorganic seed aerosol, the lumping species produced from the oxidation of HC are split into g, or and in phases by the gas-aerosol absorptive partitioning model (Pankow, 1994). The g-in partitioning coefficient ($K_{in,i}$) (m^3 μg^{-1}) are expressed as.

245 $$K_{in,i} = \frac{7.501RT}{10^9 MW_{in} \gamma_{in,i} p^{\circ}_{l,i}} \tag{Eq.3}$$

MW_{in} represents the average MW (g mol^{-1}) of inorganic phase aerosol. $p^{\circ}_{l,i}$ is the liquid vapor pressure (in mmHg) of the product i and is calculated using the group contribution method (Jang and Kamens, 1997, 1998; Zhou et al., 2019). The activity coefficient ($\gamma_{or,i}$) of organic species i in or phase is treated as one (Im et al., 2014). The activity coefficient of i in in phase ($\gamma_{in,i}$) is predicted using a semi-empirical regression equation (Zhou et al., 2019). The theoretical estimation of $\gamma_{in,i}$ was

250 conducted by using the thermodynamic Aerosol Inorganic-Organic Mixtures Functional Groups Activity Coefficients (AIOMFAC) (Zuend et al., 2011) for the given set of conditions and aerosol parameters. $\gamma_{in,i}$ is a function of aerosol environment variables (RH ranging from 0 to 1 and fractional sulfate (FS = [SO$_4^{2-}$]/[SO$_4^{2-}$]+[NH$_4^+$])) and the physicochemical parameters of lumping species i (MW$_i$, O:C$_i$, and HB$_i$) as follows,

$$\gamma_{in,i} = e^{0.035 \cdot MW_i - 2.704 \cdot \ln(O:C_i) - 1.121 \cdot HB_i - 0.330 \cdot FS - 0.022 \cdot (100 \cdot RH)} \tag{Eq.4}$$

255 Phenol can be both a donor and an accepter for hydrogen bonding while a phenoxy radical can be only a hydrogen bonding accepter. We assumed that the oxygen radical in the phenoxy radical is treated as a ketone functional group to calculate its

vapor pressure and activity coefficient. k_{off_phenol} is inversely related to the partitioning coefficient ($K_{in,i}$, Fig. 1) of species i (phenol) onto the *in* phase with the relation below,

$$k_{off\_phenol} = \frac{k_{on\_phenol}}{K_{in,phenol}} \qquad\qquad\qquad\qquad\qquad\qquad\qquad\qquad\qquad\qquad \text{(Eq.5)}$$

260   The *g-in* partitioning coefficient ($K_{in,ox,}$) of atmospheric oxidant, *ox* (i.e., H_2O_2, HONO, HO_2, OH, O_3, NO, NO_2, CH_3OOH, and CH_3CO_3H) is estimated using Henry's constant ($K_{H,i}$) below,

$$\frac{K_{H,ox}}{K_{in,ox}} = 10^6 \frac{M_{in}}{V_{in}RT} \qquad\qquad\qquad\qquad\qquad\qquad\qquad\qquad\qquad\qquad \text{(Eq.6)}$$

M_{in} (g L^{-1}) is the mass concentration of *in* phase, V_{in} (cm^{-3}/L) is volume mixing ratio of *in* phase when R is in 8.205×10^3 L atm mol^{-1} K^{-1}.

265   *Phenol* (*in*) in R6 further reacts with the OH radical ($OH(in)$) in *in* phase to form an intermediate adduct of phenol ($phenol\_OH\_int$ (*in*)) at reaction rate constant, k_1 (mol/L), which is determined empirically and very fast as seen below,

$$C_6H_5OH(in) + OH(in) \rightarrow phenol\_OH\_int \ (in) \qquad k_1 \quad (7E-6) \qquad\qquad\qquad \text{(R8)}$$
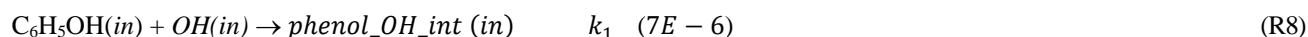
Intermediate adduct $phenol\_OH\_int$ (*in*) can effectively generate a phenoxy radical, $C_6H_5O\cdot(in)$, via an acid catalyzed reaction below.

270    $phenol\_OH\_int \ (in) \xrightarrow{H^+} C_6H_5O\cdot(in) + H_2O \qquad\qquad k_{phenoxy} \qquad\qquad\qquad\qquad \text{(R9)}$

where $k_{phenoxy} = k_1 * e^{[H^+]_{in}}$. $[H^+]_{in}$ is the proton concentration (mol/L) in aqueous phase.

In the similar manner with phenols (R6 and R7), the resulting phenoxy radical can also partition between gas and particle phases as follows:

$$C_6H_5O\cdot(g) \rightarrow C_6H_5O\cdot(in) \qquad\qquad\qquad k_{on\_phenoxy} \qquad\qquad\qquad\qquad\qquad \text{(R10)}$$

275    $C_6H_5O\cdot(in) \rightarrow C_6H_5O\cdot(g) \qquad\qquad\qquad k_{off\_phenoxy} \qquad\qquad\qquad\qquad\qquad \text{(R11)}$
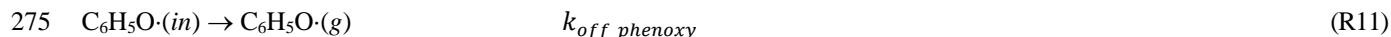
The formation of $phenol\_OH\_int$ (*in*) is the rate determining step in the mechanism. In the absence of an acid catalyst, $phenol\_OH\_int$ (*in*) can be further oxidized via the reaction with an oxygen molecule to form catechol and other multifunctional carbonyls (Xu and Wang, 2013). The produced $C_6H_5O\cdot(g)$ is involved in the reaction with ozone (R2) as seen in Fig. 2 and catalytically reduce atmospheric oxidation capacity.

280   **4. Result and Discussion**

4.1 Simulation of gas oxidation and SOA formation

Fig. 3 illustrates gas simulations (phenol, benzene, ozone, NO, and NO_2) for chamber data obtained in the UF-APHOR chamber. Overall, explicit gas simulations including HOM and H-PPR agree well with observations. In the presence of wet-inorganic seed (i.e., wet-AS, AHS, and SA), both simulations and chamber data show a significant suppression in gas

285   oxidation (i.e., ozone formation and the decay of phenol or benzene) compared to the gas oxidation in non-seeded

conditions. For example, simulations are considerably deviated from observation in both Fig. 3(B) and (H) when simulations are performed with gas mechanisms excluding the H-PPR mechanism for phenol and benzene oxidation in the presence of SA seed–. Under the same experimental conditions, simulations with H-PPR in Fig. 3(C) and (I) well predict chamber data showing the importance of H-PPR (reactions R3-R5). In addition to phenol, catechols and nitrophenols, which are major products from phenol oxidation, can also undergo the PPR formation. The suppressed ozone can lessen the production of an OH radical and further retard the aging of organic products.

Fig. 4(A-P) shows chamber-generated SOA mass from the photooxidation of phenol (Fig. 4(A-H)) or benzene (Fig.4(I-P)) in different inorganic seed conditions (Table 1) and the simulations of SOA formation using the UNIPAR model. Non-seed phenol SOA is shown in Fig. 4(A) and (B) and non-seed benzene in Fig. 4(I) and (J). SOA masses produced in the presence of inorganic seed (SA, AHS, wet- or dry-AS) are depicted in Fig. 4 (C-H) for phenol and Fig. 4 (K-P) for benzene. Overall, the improved SOA simulation of phenol or benzene was also performed with the improved gas simulation incorporated with HOM and H-PPR.

The importance of H-PPR mechanisms on SOA prediction is demonstrated in Fig. 4(C) and (G) for phenol and Fig. 4(K) and (O) for benzene by comparing simulations with H-PPR and those without H-PPR. The suppression of SOA formation was effective with acidic aerosol. Additionally, the formation rate of PPR can be influenced by the chemical property of the aerosol medium. For example, Mitroka et al. (Mitroka et al., 2010) reported that reactivity of the OH radical is considerably higher in polar, protic solvent than that in dipolar, aprotic solvent. Protic solvent is a hydrogen bond donor that stabilizes the transition state of the OH radical addition reaction. Thus, the reaction of phenols with the OH radical is more favorable in *in* phase than *or* phase. The reported radical scavenging ability of phenols by forming PPR is in the order of 1,2,3-trihydroxybenzene > 1,2,4-trihydroxybenzene > catechol (1,2-dihydroxybenzene) > 1.4-dihydroxybenzene > 1,3-dihydroxybenzene ≈ 1,3,5-trihydroxybenezene (Thavasi et al., 2009). The phenol oxidation can produce various multi-functional phenols. As shown in reaction R8, phenol in salted aqueous media reacts with $OH(in)$ in a similar way with the OH addition to the aromatic ring in the gas phase to form intermediate product $phenol\_OH\_int$ (in) (Fig. 2). Fig. S3 is the proposed mechanism to form phenoxy radical via the acid-catalyzed reaction. In addition, some organic products such as quinones can promote increased oxidants in aqueous acidic media. Quinones are well recognized for their ability to promote superoxide formation (Guin et al., 2011). Lowering pH increases the redox potential (Walczak et al., 1997) of quinone-hydroquinone. However, the reduction potential of oxygen can be lower in acidic condition and is advantageous for $O_2^{\bullet-}$ /$HO_2\bullet$ formation (Wei et al., 2022) (Section S4).

The importance of HOM on phenol SOA has been demonstrated in the previous study by Choi and Jang (Choi and Jang, 2022). For example, a large fraction of OM_P in Fig. 4(A) is contributed by HOM. The contribution of HOM to SOA mass increases with decreasing NO levels. The systematic evaluation of the UNIPAR model integrated with the explicit gas mechanisms is performed via the model sensitivity to various environmental variables (i.e., NO_x levels, seed, temperature, and humidity) in section 4.2.

 4.2 Sensitivity of SOA Formation to Environmental Variables

4.2.1 Evaluation of the impact of H-PPR on SOA Formation: aerosol acidity

In order to assess the impact of H-PPR on phenolic SOA and benzene SOA, the UNIPAR simulation was performed as a function of aerosol acidity (FS value) as seen in Fig. 5. This sensitivity was performed under the given conditions: temperature = 298 K, NO_x level = 7.5 ppbC/ppb, and RH = 0.6 at the sunlight conditions on October 19, 2022 (Fig. S1). All seeds are wet under this RH (Peng et al., 2022). The concentration of the initial HCs for each simulation was set to 30 ppb at four different HC compositions in Fig. 5: (A) phenol; (B)benzene; (C) phenol:benzene = 3:1 ppb/ppb, and (D) phenol:benzene = 1:1 ppb/ppb. The concentrations of consumed phenol or consumed benzene varied according to the different rate constant of each HC with the OH radical and the H-PPR degree.

The DSMACC box model flatform of this study is equipped with the integrated reaction rate (IRR) analysis technique, which can show the chemical reaction flow in the oxidation mechanisms. Based on the IRR analysis, the production of PPR is contributed mainly by the reaction of phenol with OH radicals in gas phase and the catechol H-PPR mechanism. The phenoxy radical production via phenol's H-PPR path is trivial due to the low partitioning of phenol into the aqueous phase. Unlike phenol, catechol, a major product of phenol oxidation, can yield the semiquinone radical (PPR of catechol) via the heterogeneous reaction mechanism. For example, in the presence of SA seed (Fig. 5(A)), the contribution of catechol's H-PPR path is 1.22 times greater than that of the gas-phase reaction of phenol with OH radicals. In the presence of wet-AS seed, the contribution of catechol's H-PPR path is 20% of that from the gas-phase reaction of phenol with OH radicals.

In Fig. 5, a considerable difference was identified between the SOA mass simulated with H-PPR (solid line) and that without H-PPR (dashed line). SOA growth is suppressed with H-PPR. This gap gradually increases with increasing aerosol acidity (FS). The reduction in SOA mass with acidic seed mainly is caused by the retardation of gas oxidation, which is linked to the catalytic consumption of ozone and , which is consequently connected to the slow oxidation of phenol (i.e., Figs 3B and 3C) and or benzene (i.e., Figs 3H and 3I)slow aging of oxygenated products (i.e., Figs 3B and 3C) or benzene (i.e., Figs 3H and 3I). The simulation also depicts the impact of the amount of inorganic seed on SOA formation of phenol or benzene. Surprisingly, phenol SOA mass is lower with the 30 μg/m³ of inorganic seed than that with 5 μg/m³ of inorganic seed, in contrast to the typical tendency in the SOA formation from non-phenolic HCs.

Compared to phenol (Fig. 5(A)), the impact of H-PPR on benzene SOA formation is small as seen in Fig. 5(B). Benzene is more affected by acid-catalyzed oligomerization than phenol. Benzene oxidation yields various products other than phenol. Some reactive organic products are involved in oligomerization in aqueous phase. As seen Fig. 5(C) and (D), when benzene is mixed with phenol in the presence of the high concentration of wet seed, SOA growth shows more suppression suggesting the impact of PPR from phenol. The SOA mass difference due to the H-PPR mechanism is large in the mixture of phenol and benzene. The smaller amount of phenol consumption in the gas mixture as seen in Fig. 5(C) and (D) yields less SOA mass, which impacts partitioning of products and their oligomerization in aerosol. Thus, the impact of H-PPR on SOA mass in Fig. 5(C) and (D) is relatively more significant than that in Fig. 5(A) due to the difference in SOA yields. —These

simulation results suggest that phenolic compounds in biomass burning smoke gases might impact the atmospheric oxidation ability of urban air.

4.2.2 Sensitivity of SOA formation to NO_x level, Temperature, and RH

Fig. 6 (6A-6D) displays the sensitivity of the SOA mass to NO_x levels at three different temperatures (278 K, 288 K and 298 K) and two different seed conditions (no seed and AHS seed at RH = 0.6). Fig. 7 illustrates the sensitivity of phenol or benzene SOA mass to RH (0.3 and 0.6) at two different seed conditions (AHS and AS seed). The UNIPAR simulation was evaluated at the given sunlight conditions on October 19, 2022 (between 6:30 AM to 5:30 PM EST, Fig. S1). The initial concentration of HCs in each simulation in Figs. 6 and 7 was set to 30 ppb to mimic the real-world condition.

A typical negative correlation appears between SOA mass and temperature (Fig. 6). Regardless of seed conditions, a typical NO_x impact on SOA formation appears at high NO_x regions (HC ppbC/NO_x $\leq$ 5) showing a negative correlation between NO_x levels and SOA formation. At the higher NO_x level, more organonitrate forms via the reaction of peroxy radicals with NO. Organonitrates attribute to SOA formation mainly via the partitioning process and their volatility is relatively high (Choi and Jang, 2022). Phenol SOA is more sensitive to the NO_x level than benzene SOA. As the NO_x level decreases in low NO_x regions (HC ppbC/NO_x > 5), SOA production gradually increases because of the increased contribution of low-volatile multi-hydroxyl products (HOM products that form via multiple additions of OH radicals into phenol) in the absence of wet seed (Fig. 6(A) and 6(C). Thus, the increased HOM products at the low NO_x level decrease the sensitivity of SOA formation to temperature. In the presence of acidic seed, the production of phenoxy radicals increases with decreasing NO_x levels due to increased oxidants in aerosol phase, and negatively influences SOA formation.

Phenol rapidly reacts with OH radicals (2.82 10^{-11} cm^3 molecule^{-1} s^{-1} at 298 K) (Kwok and Atkinson, 1995; Yee et al., 2013) in the gas phase and quickly produces low volatile products compared to benzene (1.2 10^{-12} cm^3 molecule^{-1} s^{-1} at 298 K) (Kwok and Atkinson, 1995). Thus, phenol produces a higher SOA mass than benzene at given simulation conditions (at the same initial HC concentration, NO_x levels, and sunlight). The reaction rate of benzene with the OH radical is even slower than that of NO_2 with the OH radical. Nearly 47% of benzene oxidation would form gas-oxidation products other than phenol and some of them can be involved in aerosol phase oligomerization. Benzene SOA yields can be significant although benzene decay is slow (Fig. 3 and Fig. 4).

Of the total PPR production, the contribution of daytime phenol oxidation with nitrate radicals is only 0.1% of that from the phenol oxidation with OH radicals in the high NO_x condition (VOC ppbC/NO_x ppb = 2) of Fig. 6(**B**). However, the contribution of nitrate radical mechanism to form PPR increases in the absence of sunlight. For example, the contribution of nitrate radicals on PPR is nearly 30% of that with OH radicals at a given simulation condition under the high NO_x condition between 4PM to 5PM (Fig. 6(A)). This simulation result suggests that the nitrate radical oxidation with phenol is important to form PPR during nighttime.

AS seed in Fig. 7(A) can be effloresced at RH 0.35-0.4. Thus, AS-seed is dry at RH= 0.3 but wet at RH = 0.6. Fig. 7(A) displays a higher SOA formation at 0.6 RH than 0.3 RH because of aqueous phase oligomerization (Choi and Jang, 2022;

Han and Jang, 2022, 2023; Im et al., 2014; Yu et al., 2021b; Zhou et al., 2019; Yu et al., 2021a). Overall, both phenol and benzene SOA are slightly sensitive to RH conditions. In the presence of AHS seed that is wet in both RHs (0.3 and 0.6), both phenol and benzene exhibit an unusual tendency showing higher SOA mass with lower RH. SOA growth from both benzene and phenol can increase due to acid-catalyzed oligomerization but it can also be partly suppressed via the H-PPR

390 mechanism. Fig. 7(B) and 7(C) display OM_{AR} (oligomeric SOA mass) and OM_P (partitioning mass) contributions to OM_T. Both benzene and phenol SOA are dominated by OM_{AR} at given simulation conditions.

4.3. Uncertainty of SOA Formation to Model Parameters

Fig. 8 illustrates the uncertainties of important model parameters in predicting SOA mass using the UNIPAR model. The partitioning process (OM_P) is most impacted by the lumping species' vapor pressure (VP). OM_{AR} is influenced by the

395 reaction rates of oligomerization of the reactive lumping species ($k_{oligomerization}$) and H-PPR ($k_{phenoxy}$). The uncertainties of the estimated VP are set to the reported value associated with the group contribution method (Zhao et al., 1999; Yu et al., 2021b). The corresponding change in the SOA mass owing to VP uncertainties ranges from -20% to 24% in benzene SOA simulation with wet-AS seed at given simulation conditions (Fig. 8(A)). Under the same condition, the change in the phenol SOA mass due to VP uncertainties ranges from -13% to 14%. Benzene SOA (Fig. 8(A)) is more sensitive to the VP

400 uncertainty than phenol SOA (Fig. 8(B)). As seen in Fig. 8C and 8D, SOA mass is more significantly impacted by the uncertainty associated with the oligomerization rate constant than that of the H-PPR rate constant at a given uncertainty range. The variation in SOA formation with the change of $k_{phenoxy}$ is trivial. For H-PPR, the amount of available oxidants (i.e., OH radicals, HONO, and H_2O_2) is more critical than $k_{phenoxy}$ in our model.

5. Conclusion and Atmospheric Implications

405 Hitherto, the typical role of inorganic acids was known to be an acid catalyst that can accelerate the oligomerization of reactive organic species (i.e., aldehydes and epoxide) in aerosol phase (Jang et al., 2002; Garland et al., 2006; Hallquist et al., 2009). SOA growth accelerated by an acid catalyst has been reported in various chamber studies including both aromatic and biogenic HCs. Surprisingly, the acidic aerosol along with phenol and benzene suppressed the oxidation of air including ozone formation and the decay of HCs (Fig. 3) due to the heterogeneous formation of PPR.

410 The gas mechanisms including formation of HOM and H-PPR simulated well gas oxidation (i.e., ozone, NO_x and the decay of benzene or phenol) and improved the prediction of SOA formation using UNIPAR (Fig. 4). As seen in Fig. 5, phenol SOA still increases via heterogeneous oligomerization showing a difference in SOA mass between dry- and wet-AS seed. As discussed in Section 3.2.2, the heterogeneously produced PPR production occurs via the reaction of phenolic compounds with the aerosol-phase OH radical that is available during daytime due to the photolysis of H_2O_2 and HONO. Thus, the

415 heterogeneously produced PPR is effective with wet-inorganic aerosol during the daytime.

Fundamentally, biomass burning under open flame is performed at low temperatures and produces very low NO (Simoneit, 2002; Mebust and Cohen, 2013; Xu et al., 2021). The chemistry slows to a standstill without NO_x and thus halts ozone formation although gaseous HCs are abundant. When these fire plumes mix into urban atmospheres abundant in NO_x, ozone formation becomes active, impacting the air quality of the city. Chamber data of this study mimic the phenol oxidation in the presence of NO_x. In addition, hygroscopic inorganic aerosols comprising of nitrate, sulfate and ammonium ions are available in the city environment rich in NO_x, SO_2 and NH_3. When wildfire plumes mix in city air, their phenolic compounds interact with NO_x and hygroscopic inorganic aerosol. The results from this study suggest that PPR produced during the atmospheric process of phenolic compounds in wildfire plumes can temporarily retard the atmospheric oxidation in urban environments. The SOA simulation with the low concentrations of phenol and typical atmospheric tracer gases (formaldehyde, acetaldehyde) in Fig. 5 shows that phenol SOA is considerably suppressed even with a small amount of wet inorganic aerosol raging from weakly to neutral acidity. For example, phenol SOA mass decreases by 12% with 5 ppb of ammonium hydrogen sulfate (FS=0.5) (Fig. 5(A)) and the SOA mass from the mixture of phenol and benzene decreased by 28% (Fig. 5(C)).

The impact of NO_x on SOA formation appears to be negative under high NO_x levels as shown in Fig. 6. A significant fraction of phenolic SOA forms through HOM and oligomeric matter. The contribution of HOM and oligomeric matter on SOA formation is generally higher with the lower NO_x level. Thus, phenol or benzene SOA at the NO_x-limit condition is relatively insensitive to temperature (Fig. 6) due to the formation of nonvolatile products. Similarly, SOA from biomass burning might be insignificantly affected by temperature under low NO_x regimes. When the concentrations of NO_x drop in the high NO_x regime, SOA formation increases. The role of PPR on atmospheric oxidation capacity in the blending of wildfire smoke and urban pollutants needs to be studied under different NO_x levels.

A variety of phenolic compounds including phenol, cresol, catechol, methoxyphenols, dimethylphenols (Akherati et al., 2020; Bruns et al., 2016) can consist of more than 80% of the precursor HCs in wildfire smoke. These multifunctional phenolic compounds can also yield PPR as active scavengers for ozone (Section 3.2.2). To date, the impact of phenolic compounds on retardation of atmospheric aging of HCs in the city air has not been sufficiently studied. It is important to comprehend the formation mechanisms of PPR-like chemical species and their role on atmospheric oxidation capability to accurately predict the elevation of ozone and SOA as well as their peak time.

Several unresolved issues need to address to accurately predict SOA formation from biomass burning smoke, including gas mechanisms of unidentified HCs in wildfire smoke, the role of the aqueous phase on the formation of PPR, and unidentified SOA formation mechanisms. For example, there are still missing mechanisms, including cross-reactions of RO_2 radicals and the distribution of oxidation paths. This study focused on the oxidation of phenol and benzene through their reaction with OH radicals. Ozone, which mainly forms during daytime, often persists through the night and reacts with NO_2 to form nitrate radicals at night. Phenol can react with this nitrate radical during the night although its reaction is slower than that with OH radical. The reaction of phenols with nitrate radical can also produce PPR-like species and can catalytically scavenge ozone. Nighttime humidity, which increases as temperature decreases, can surpass delinquent RH (DRH) of

450 hygroscopic inorganic constituents and form wet inorganic aerosol. The resulting aerosol can be wet until humidity drops

below ERH. To better predict SOA formation, the atmospheric processes of biomass burning smoke needs to be studied

under different climate conditions, such as temperature, humidity, and sunlight, and emissions of air pollutants.

Phenol is the most abundant first-generation product from the oxidation of benzene (Smith et al., 2014; Johnson et al., 2004).

Additionally, the formation of cresol is involved in 18% of toluene-OH reactions. Xu et al. explained that toluene SOA

455 formation was underestimated by about 20% proposing the uncertainty in the formation of phenolic compounds (Xu et al.,

2015). Dimethylphenols can also be produced from the oxidation of xylenes. Comprehension of the atmospheric process of

phenolic compounds can improve the prediction of SOA formation from aromatic HCs. A large fraction of phenolic

compounds is directly emitted but its impact on SOA mass is missing in the current air quality model (Pye et al., 2023).

Acknowledgments

460 This research was supported by the National Institute of Environmental Research (NIER2020-01-01-010); the National

Science Foundation (AGS1923651); the LG Electronics Inc. (C2023007555); and the Fine Particle Research Initiative in

East Asia Considering National Differences (FRIEND) Project through the National Research Foundation of Korea (NRF)

funded by the Ministry of Science and ICT (2020M3G1A1114556).

465 Data availability. Chamber simulation data is available upon request.

Author contributions. JC and MJ conducted chamber experiments and simulated the UNIPAR SOA model. JC, MJ, and SB

processed chamber data.

470 Competing interest. The authors declare that they have no conflict of interest.

References

Akherati, A., He, Y., Coggon, M. M., Koss, A. R., Hodshire, A. L., Sekimoto, K., Warneke, C., de Gouw, J., Yee, L., Seinfeld, J. H., Onasch, T. B., Herndon, S. C., Knighton, W. B., Cappa, C. D., Kleeman, M. J., Lim, C. Y., Kroll, J. H.,
475 Pierce, J. R., and Jathar, S. H.: Oxygenated Aromatic Compounds are Important Precursors of Secondary Organic Aerosol in Biomass-Burning Emissions, Environmental Science & Technology, 54, 8568-8579, 10.1021/acs.est.0c01345, 2020.
Atkinson, R.: Atmospheric chemistry of VOCs and NO_x, Atmos. Environ., 34, 2063-2101, 2000.
Beardsley, L. R. and Jang, M.: Simulating the SOA formation of isoprene from partitioning and aerosol phase reactions in the presence of inorganics, Atmospheric Chemistry and Physics, 16, 5993-6009, 10.5194/acp-16-5993-2016, 2016.
480 Bloss, C., Wagner, V., Jenkin, M. E., Volkamer, R., Bloss, W. J., Lee, J. D., Heard, D. E., Wirtz, K., Martin-Reviejo, M., Rea, G., Wenger, J. C., and Pilling, M. J.: Development of a detailed chemical mechanism (MCMv3.1) for the atmospheric oxidation of aromatic hydrocarbons, Atmos. Chem. Phys., 5, 641-664, 2005.
Borrás, E. and Tortajada-Genaro, L. A.: Secondary organic aerosol formation from the photo-oxidation of benzene, Atmospheric Environment, 47, 154-163, https://doi.org/10.1016/j.atmosenv.2011.11.020, 2012.

485   Brown, H. C. and Okamoto, Y.: Electrophilic Substituent Constants, Journal of the American Chemical Society, 80, 4979-4987, 10.1021/ja01551a055, 1958.

Bruns, E. A., El Haddad, I., Slowik, J. G., Kilic, D., Klein, F., Baltensperger, U., and Prévôt, A. S. H.: Identification of significant precursor gases of secondary organic aerosols from residential wood combustion, Scientific Reports, 6, 27881, 10.1038/srep27881, 2016.

490   Calvert, J. G., Atkins, R., Becker, K. H., Kamens, R. M., Seinfeld, J. H., Wallington, T. J., and Yarwood, G.: Mechanisms of atmospheric oxidation of aromatic hydrocarbons, Reactions of aromatic compounds with OH radicals (Chap. 2), Oxford University Press, New York2002.

Cao, G. and Jang, M.: Effects of particle acidity and UV light on secondary organic aerosol formation from oxidation of aromatics in the absence of NO_x, Atmos. Environ., 35, 7603-7613, 2007.

495   Carlton, A. G., Bhave, P. V., Napelenok, S. L., Edney, E. O., Sarwar, G., Pinder, R. W., Pouliot, G. A., and Houyoux, M.: Model Representation of Secondary Organic Aerosol in CMAQv4.7, Environ. Sci. Technol., 44, 8553-8560, 10.1021/es100636q, 2010.

Carter, W. P. and Atkinson, R.: Alkyl nitrate formation from the atmospheric photoxidation of alkanes; a revised estimation method, Journal of atmospheric chemistry, 8, 165-173, 1989.

500   Carter, W. P. L.: Development of Ozone Reactivity Scales for Volatile Organic Compounds, Air & Waste, 44, 881-899, 10.1080/1073161X.1994.10467290, 1994.

Choi, J. and Jang, M.: Suppression of the Phenolic SOA formation in the Presence of Electrolytic Inorganic Seed, Journal: Science of the Total Environment, 851, 158082, 2022.

Das, T. N.: Oxidation of Phenol in Aqueous Acid: Characterization and Reactions of Radical Cations vis-à-vis the Phenoxyl

505   Radical, The Journal of Physical Chemistry A, 109, 3344-3351, 10.1021/jp050015p, 2005.

Deng, Y., Inomata, S., Sato, K., Ramasamy, S., Morino, Y., Enami, S., and Tanimoto, H.: Temperature and acidity dependence of secondary organic aerosol formation from α-pinene ozonolysis with a compact chamber system, Atmos. Chem. Phys., 21, 5983-6003, 10.5194/acp-21-5983-2021, 2021.

Dixon, W. T. and Murphy, D.: Determination of the acidity constants of some phenol radical cations by means of electron

510   spin resonance, Journal of the Chemical Society, Faraday Transactions 2: Molecular and Chemical Physics, 72, 1221-1230, 10.1039/F29767201221, 1976.

Edwards, D. P., Emmons, L. K., Gille, J. C., Chu, A., Attié, J.-L., Giglio, L., Wood, S. W., Haywood, J., Deeter, M. N., Massie, S. T., Ziskin, D. C., and Drummond, J. R.: Satellite-observed pollution from Southern Hemisphere biomass burning, Journal of Geophysical Research: Atmospheres, 111, https://doi.org/10.1029/2005JD006655, 2006.

515   Emmerson, K. M. and Evans, M. J.: Comparison of tropospheric gas-phase chemistry schemes for use within global models, Atmos. Chem. Phys., 9, 1831-1845, 10.5194/acp-9-1831-2009, 2009.

Finlayson-Pitts, B. J. and Pitts, J. N.: Chemistry of the upper and lower atmosphere: Theory, Experiments, and Applications, Academic Press, New York2000.

Garland, R. M., Elrod, M. J., Kincaid, K., Beaver, M. R., Jimenez, J. L., and Tolbert, M. A.: Acid-catalyzed reactions of

520   hexanal on sulfuric acid particles: Identification of reaction products, Atmos. Environ., 40, 6863-6878, 2006.

Garmash, O., Rissanen, M. P., Pullinen, I., Schmitt, S., Kausiala, O., Tillmann, R., Zhao, D., Percival, C., Bannan, T. J., Priestley, M., Hallquist, Å. M., Kleist, E., Kiendler-Scharr, A., Hallquist, M., Berndt, T., McFiggans, G., Wildt, J., Mentel, T. F., and Ehn, M.: Multi-generation OH oxidation as a source for highly oxygenated organic molecules from aromatics, Atmos. Chem. Phys., 20, 515-537, 10.5194/acp-20-515-2020, 2020.

525   Guin, P. S., Das, S., and Mandal, P. C.: Electrochemical Reduction of Quinones in Different Media: A Review, International Journal of Electrochemistry, 2011, 816202, 10.4061/2011/816202, 2011.

Hallquist, M., Wenger, J. C., Baltensperger, U., Rudich, Y., Simpson, D., Claeys, M., Dommen, J., Donahue, N. M., George, C., Goldstein, A. H., Hamilton, J. F., Herrmann, H., Hoffmann, T., Iinuma, Y., Jang, M., Jenkin, M. E., Jimenez, J. L., Kiendler-Scharr, A., Maenhaut, W., McFiggans, G., Mentel, T. F., Monod, A., Prévôt, A. S. H., Seinfeld, J. H., Surratt, J. D.,

530   Szmigielski, R., and Wildt, J.: The formation, properties and impact of secondary organic aerosol: current and emerging issues, Atmos. Chem. Phys., 9, 5155-5236, 2009.

Han, S. and Jang, M.: Modeling Diurnal Variation of SOA Formation via Multiphase Reactions of Biogenic Hydrocarbons, Atmos. Chem. Phys. Discuss., 2022, 1-25, 10.5194/acp-2022-327, 2022.

Han, S. and Jang, M.: Modeling daytime and nighttime secondary organic aerosol formation via multiphase reactions of biogenic hydrocarbons, Atmos. Chem. Phys., 23, 1209-1226, 10.5194/acp-23-1209-2023, 2023.

Hansch, C., McKarns, S. C., Smith, C. J., and Doolittle, D. J.: Comparative QSAR evidence for a free-radical mechanism of phenol-induced toxicity, Chemico-biological interactions, 127, 61-72, 10.1016/s0009-2797(00)00171-x, 2000.

Holton, D. M. and Murphy, D.: Determination of acid dissociation constants of some phenol radical cations. Part 2, Journal of the Chemical Society, Faraday Transactions 2: Molecular and Chemical Physics, 75, 1637-1642, 10.1039/F29797501637, 1979.

Hudson, P. K., Murphy, D. M., Cziczo, D. J., Thomson, D. S., de Gouw, J. A., Warneke, C., Holloway, J., Jost, H.-J., and Hübler, G.: Biomass-burning particle measurements: Characteristic composition and chemical processing, Journal of Geophysical Research: Atmospheres, 109, https://doi.org/10.1029/2003JD004398, 2004.

Im, Y., Jang, M., and Beardsley, R.: Simulation of Aromatic SOA Formation Using the Lumping Model Integrated with Explicit Gas-Phase Kinetic Mechanisms and Aerosol Phase Reactions, Atmos. Chem. Phys. , 13, 5843-5870, 10.5194/acp-14-4013-2014, 2014.

Jagiella, S. and Zabel, F.: Reaction of phenylperoxy radicals with NO 2 at 298 K, Physical Chemistry Chemical Physics, 9, 5036-5051, 2007.

Jang, M. and Kamens, R. M.: Application of group contribution methods to the partitioning of semi-volatile organic compounds on atmospheric particulate matter, 771-781,

Jang, M. and Kamens, R. M.: A Thermodynamic Approach for Modeling Partitioning of Semivolatile Organic Compounds on Atmospheric Particulate Matter: Humidity Effects, Environ. Sci. Technol., 32, 1237-1243, 1998.

Jang, M., Czoschke, N. M., Lee, S., and Kamens, R. M.: Heterogeneous Atmospheric Aerosol Production by Acid-Catalyzed Particle-Phase Reactions, Science, 298, 814-817, 2002.

Jenkin, M. E., Derwent, R. G., and Wallington, T. J.: Photochemical ozone creation potentials for volatile organic compounds: Rationalization and estimation, Atmospheric Environment, 163, 128-137, https://doi.org/10.1016/j.atmosenv.2017.05.024, 2017.

Jenkin, M. E., Saunders, S. M., Wagner, V., and Pilling, M. J.: Protocol for the development of the master chemical mechanism, MCM v3 (part B): tropospheric degradation of aromatic volatile organic compounds, Atmospheric Chemistry and Physics, 3, 181-193, 2003.

Ji, Y., Zhao, J., Terazono, H., Misawa, K., Levitt, N. P., Li, Y., Lin, Y., Peng, J., Wang, Y., Duan, L., Pan, B., Zhang, F., Feng, X., An, T., Marrero-Ortiz, W., Secrest, J., Zhang, A. L., Shibuya, K., Molina, M. J., and Zhang, R.: Reassessing the atmospheric oxidation mechanism of toluene, Proc Natl Acad Sci U S A, 114, 8169-8174, 10.1073/pnas.1705463114, 2017.

Jimenez, J. L., Canagaratna, M. R., Donahue, N. M., Prevot, A. S. H., Zhang, Q., Kroll, J. H., DeCarlo, P. F., Allan, J. D., Coe, H., Ng, N. L., Aiken, A. C., Docherty, K. S., Ulbrich, I. M., Grieshop, A. P., Robinson, A. L., Duplissy, J., Smith, J. D., Wilson, K. R., Lanz, V. A., Hueglin, C., Sun, Y. L., Tian, J., Laaksonen, A., Raatikainen, T., Rautiainen, J., Vaattovaara, P., Ehn, M., Kulmala, M., Tomlinson, J. M., Collins, D. R., Cubison, M. J., Dunlea, J., Huffman, J. A., Onasch, T. B., Alfarra, M. R., Williams, P. I., Bower, K., Kondo, Y., Schneider, J., Drewnick, F., Borrmann, S., Weimer, S., Demerjian, K., Salcedo, D., Cottrell, L., Griffin, R., Takami, A., Miyoshi, T., Hatakeyama, S., Shimono, A., Sun, J. Y., Zhang, Y. M., Dzepina, K., Kimmel, J. R., Sueper, D., Jayne, J. T., Herndon, S. C., Trimborn, A. M., Williams, L. R., Wood, E. C., Middlebrook, A. M., Kolb, C. E., Baltensperger, U., and Worsnop, D. R.: Evolution of Organic Aerosols in the Atmosphere, Science (Washington, DC, United States), 326, 1525-1529, 10.1126/science.1180353, 2009.

Johnson, D., Jenkin, M. E., Wirtz, K., and Martin-Reviejo, M.: Simulating the Formation of Secondary Organic Aerosol from the Photooxidation of Toluene, Environmental Chemistry, 1, 150-165, https://doi.org/10.1071/EN04069, 2004.

Kanakidou, M., Seinfeld, J. H., Pandis, S. N., Barnes, I., Dentener, F. J., Facchini, M. C., Van Dingenen, R., Ervens, B., Nenes, A., Nielsen, C. J., Swietlicki, E., Putaud, J. P., Balkanski, Y., Fuzzi, S., Horth, J., Moortgat, G. K., Winterhalter, R., Myhre, C. E. L., Tsigaridis, K., Vignati, E., Stephanou, E. G., and Wilson, J.: Organic aerosol and global climate modelling: A review, Atmos. Chem. Phys., 5, 1053-1123, 10.5194/acp-5-1053-2005, 2005.

Kwok, E. S. C. and Atkinson, R.: Estimation of hydroxyl radical reaction rate constants for gas-phase organic compounds using a structure-reactivity relationship: an update, Atmos. Environ., 29, 1685-1695, 10.1016/1352-2310(95)00069-b, 1995.

Li, J., Jang, M., and Beardsley, R.: Dialkylsulfate Formation in Sulfuric Acid Seeded Secondary Organic Aerosol Produced Using an Outdoor Chamber Under Natural Sunlight, Environmental Chemistry, 13, 590-601, 10.1071/EN15129, 2015.

Liggio, J., Li, S.-M., and McLaren, R.: Reactive uptake of glyoxal by particulate matter, J.Geophy. Res., 110, D10304-10301-D10304/10313, 2005.

585 Majdi, M., Sartelet, K., Lanzafame, G. M., Couvidat, F., Kim, Y., Chrit, M., and Turquety, S.: Precursors and formation of secondary organic aerosols from wildfires in the Euro-Mediterranean region, Atmospheric Chemistry and Physics, 19, 5543-5569, 2019.

Mebust, A. K. and Cohen, R. C.: Observations of a seasonal cycle in NO_x emissions from fires in African woody savannas, Geophysical Research Letters, 40, 1451-1455, https://doi.org/10.1002/grl.50343, 2013.

590 Mitroka, S., Zimmeck, S., Troya, D., and Tanko, J. M.: How solvent modulates hydroxyl radical reactivity in hydrogen atom abstractions, J Am Chem Soc, 132, 2907-2913, 10.1021/ja903856t, 2010.

Mvula, E., Schuchmann, M. N., and von Sonntag, C.: Reactions of phenol-OH-adduct radicals. Phenoxyl radical formation by water elimination vs. oxidation by dioxygen, Journal of the Chemical Society, Perkin Transactions 2, 264-268, 10.1039/B008434O, 2001.

595 Nakao, S., Clark, C., Tang, P., Sato, K., and Cocker Iii, D.: Secondary organic aerosol formation from phenolic compounds in the absence of NO_x, Atmos. Chem. Phys., 11, 10649-10660, 10.5194/acp-11-10649-2011, 2011.

Ng, N. L., Chhabra, P. S., Chan, A. W. H., Surratt, J. D., Kroll, J. H., Kwan, A. J., McCabe, D. C., Wennberg, P. O., Sorooshian, A., Murphy, S. M., Dalleska, N. F., Flagan, R. C., and Seinfeld, J. H.: Effect of NO_x level on secondary organic aerosol (SOA) formation from the photooxidation of terpenes, Atmos. Chem. Phys., 7, 5159-5174, 2007.

600 Olmez-Hanci, T. and Arslan-Alaton, I.: Comparison of sulfate and hydroxyl radical based advanced oxidation of phenol, Chemical Engineering Journal, 224, 10-16, https://doi.org/10.1016/j.cej.2012.11.007, 2013.

Pankow, J. F.: An absorption model of the gas/aerosol partitioning involved in the formation of secondary organic aerosol, Atmos. Environ., 28, 189-193, 1994.

Peng, C., Chen, L., and Tang, M.: A database for deliquescence and efflorescence relative humidities of compounds with
605 atmospheric relevance, Fundamental Research, 2, 578-587, https://doi.org/10.1016/j.fmre.2021.11.021, 2022.

Pillar-Little, E. A., Zhou, R., and Guzman, M. I.: Heterogeneous Oxidation of Catechol, The Journal of Physical Chemistry A, 119, 10349-10359, 10.1021/acs.jpca.5b07914, 2015.

Pye, H. O. T., Place, B. K., Murphy, B. N., Seltzer, K. M., D'Ambro, E. L., Allen, C., Piletic, I. R., Farrell, S., Schwantes, R. H., Coggon, M. M., Saunders, E., Xu, L., Sarwar, G., Hutzell, W. T., Foley, K. M., Pouliot, G., Bash, J., and Stockwell, W.
610 R.: Linking gas, particulate, and toxic endpoints to air emissions in the Community Regional Atmospheric Chemistry Multiphase Mechanism (CRACMM), Atmos. Chem. Phys., 23, 5043-5099, 10.5194/acp-23-5043-2023, 2023.

Reche, C., Viana, M., Amato, F., Alastuey, A., Moreno, T., Hillamo, R., Teinilä, K., Saarnio, K., Seco, R., Peñuelas, J., Mohr, C., Prévôt, A. S. H., and Querol, X.: Biomass burning contributions to urban aerosols in a coastal Mediterranean City, Science of The Total Environment, 427-428, 175-190, https://doi.org/10.1016/j.scitotenv.2012.04.012, 2012.

615 Schell, B., Ackermann, I. J., Hass, H., Binkowski, F. S., and Ebel, A.: Modeling the formation of secondary organic aerosol within a comprehensive air quality model system, Journal of Geophysical Research, [Atmospheres], 106, 28275-28293, 2001.

Schill, G. P., Froyd, K. D., Bian, H., Kupc, A., Williamson, C., Brock, C. A., Ray, E., Hornbrook, R. S., Hills, A. J., Apel, E. C., Chin, M., Colarco, P. R., and Murphy, D. M.: Widespread biomass burning smoke throughout the remote troposphere,
620 Nature Geoscience, 13, 422-427, 10.1038/s41561-020-0586-1, 2020.

Simoneit, B. R. T.: Biomass burning — a review of organic tracers for smoke from incomplete combustion, Applied Geochemistry, 17, 129-162, https://doi.org/10.1016/S0883-2927(01)00061-0, 2002.

Smith, J. D., Sio, V., Yu, L., Zhang, Q., and Anastasio, C.: Secondary Organic Aerosol Production from Aqueous Reactions of Atmospheric Phenols with an Organic Triplet Excited State, Environmental Science & Technology, 48, 1049-1057,
625 10.1021/es4045715, 2014.

Steadman, J. and Syage, J. A.: Picosecond studies of proton transfer in clusters. 2. Dynamics and energetics of solvated phenol cation, Journal of the American Chemical Society, 113, 6786-6795, 10.1021/ja00018a011, 1991.

Sun, Q., Tripathi, G. N. R., and Schuler, R. H.: Time-resolved resonance Raman spectroscopy of p-aminophenol radical cation in aqueous solution, The Journal of Physical Chemistry, 94, 6273-6277, 10.1021/j100379a023, 1990.

630 Sun, Y. L., Zhang, Q., Anastasio, C., and Sun, J.: Insights into secondary organic aerosol formed via aqueous-phase reactions of phenolic compounds based on high resolution mass spectrometry, Atmos. Chem. Phys., 10, 4809-4822, 10.5194/acp-10-4809-2010, 2010.

Surratt, J. D., Lewandowski, M., Offenberg, J. H., Jaoui, M., Kleindienst, T. E., Edney, E. O., and Seinfeld, J. H.: Effect of acidity on secondary organic aerosol formation from isoprene, Environ Sci Technol, 41, 5363-5369, 10.1021/es0704176, 2007a.

635

Surratt, J. D., Kroll, J. H., Kleindienst, T. E., Edney, E. O., Claeys, M., Sorooshian, A., Ng, N. L., Offenberg, J. H., Lewandowski, M., Jaoui, M., Flagan, R. C., and Seinfeld, J. H.: Evidence for Organosulfates in Secondary Organic Aerosol, Environ. Sci. Technol., 41, 517-527, 2007b.

Tao, Z. and Li, Z.: A kinetics study on reactions of C_6H_5O with C_6H_5O and O_3 at 298 k, International Journal of Chemical Kinetics, 31, 65-72, https://doi.org/10.1002/(SICI)1097-4601(1999)31:1<65::AID-KIN8>3.0.CO;2-J, 1999.

640

Thavasi, V., Bettens, R. P. A., and Leong, L. P.: Temperature and Solvent Effects on Radical Scavenging Ability of Phenols, The Journal of Physical Chemistry A, 113, 3068-3077, 10.1021/jp806679v, 2009.

Verma, D. K. and Tombe, K. d.: Benzene in Gasoline and Crude Oil: Occupational and Environmental Implications, AIHA Journal, 63, 225-230, 10.1080/15428110208984708, 2002.

645

Walczak, M. M., Dryer, D. A., Jacobson, D. D., Foss, M. G., and Flynn, N. T.: pH Dependent Redox Couple: An Illustration of the Nernst Equation, Journal of Chemical Education, 74, 1195, 10.1021/ed074p1195, 1997.

Wang, T., Bo, P., Bing, T., Zhaoyun, Z., Liyu, D., and Yonglong, L.: Benzene homologues in environmental matrixes from a pesticide chemical region in China: Occurrence, health risk and management, Ecotoxicology and Environmental Safety, 104, 357-364, https://doi.org/10.1016/j.ecoenv.2014.01.035, 2014.

650

Wei, J., Fang, T., and Shiraiwa, M.: Effects of Acidity on Reactive Oxygen Species Formation from Secondary Organic Aerosols, ACS Environmental Au, 2, 336-345, 10.1021/acsenvironau.2c00018, 2022.

Wohl, C., Li, Q., Cuevas, C. A., Fernandez, R. P., Yang, M., Saiz-Lopez, A., and Simó, R.: Marine biogenic emissions of benzene and toluene and their contribution to secondary organic aerosols over the polar oceans, Science Advances, 9, eadd9031, doi:10.1126/sciadv.add9031, 2023.

655

Wotawa, G. and Trainer, M.: The Influence of Canadian Forest Fires on Pollutant Concentrations in the United States, Science (New York, N.Y.), 288, 324-328, doi:10.1126/science.288.5464.324, 2000.

Xu, C. and Wang, L.: Atmospheric Oxidation Mechanism of Phenol Initiated by OH Radical, The Journal of Physical Chemistry A, 117, 2358-2364, 10.1021/jp308856b, 2013.

Xu, J., Griffin, R. J., Liu, Y., Nakao, S., and Cocker, D. R.: Simulated impact of NO_x on SOA formation from oxidation of

660

toluene and m-xylene, Atmospheric Environment, 101, 217-225, https://doi.org/10.1016/j.atmosenv.2014.11.008, 2015.

Xu, L., Crounse, J. D., Vasquez, K. T., Allen, H., Wennberg, P. O., Bourgeois, I., Brown, S. S., Campuzano-Jost, P., Coggon, M. M., Crawford, J. H., DiGangi, J. P., Diskin, G. S., Fried, A., Gargulinski, E. M., Gilman, J. B., Gkatzelis, G. I., Guo, H., Hair, J. W., Hall, S. R., Halliday, H. A., Hanisco, T. F., Hannun, R. A., Holmes, C. D., Huey, L. G., Jimenez, J. L., Lamplugh, A., Lee, Y. R., Liao, J., Lindaas, J., Neuman, J. A., Nowak, J. B., Peischl, J., Peterson, D. A., Piel, F., Richter, D.,

665

Rickly, P. S., Robinson, M. A., Rollins, A. W., Ryerson, T. B., Sekimoto, K., Selimovic, V., Shingler, T., Soja, A. J., St. Clair, J. M., Tanner, D. J., Ullmann, K., Veres, P. R., Walega, J., Warneke, C., Washenfelder, R. A., Weibring, P., Wisthaler, A., Wolfe, G. M., Womack, C. C., and Yokelson, R. J.: Ozone chemistry in western U.S. wildfire plumes, Science Advances, 7, eabl3648, doi:10.1126/sciadv.abl3648, 2021.

Yee, L. D., Kautzman, K. E., Loza, C. L., Schilling, K. A., Coggon, M. M., Chhabra, P. S., Chan, M. N., Chan, A. W. H.,

670

Hersey, S. P., Crounse, J. D., Wennberg, P. O., Flagan, R. C., and Seinfeld, J. H.: Secondary organic aerosol formation from biomass burning intermediates: phenol and methoxyphenols, Atmos. Chem. Phys., 13, 8019-8043, 10.5194/acp-13-8019-2013, 2013.

Yu, L., Smith, J., Laskin, A., George, K. M., Anastasio, C., Laskin, J., Dillner, A. M., and Zhang, Q.: Molecular transformations of phenolic SOA during photochemical aging in the aqueous phase: competition among oligomerization,

675

functionalization, and fragmentation, Atmos. Chem. Phys., 16, 4511-4527, 10.5194/acp-16-4511-2016, 2016.

Yu, Z., Jang, M., and Madhu, A.: Prediction of Phase State of Secondary Organic Aerosol Internally Mixed with Aqueous Inorganic Salts, The Journal of Physical Chemistry A, 125(47), 10198–10206, 10.1021/acs.jpca.1c06773, 2021a.

Yu, Z., Jang, M., Zhang, T., Madhu, A., and Han, S.: Simulation of Monoterpene SOA Formation by Multiphase Reactions Using Explicit Mechanisms, ACS Earth and Space Chemistry, 5, 1455-1467, 2021b.

680

Zhang, Q., Jimenez, J. L., Canagaratna, M. R., Allan, J. D., Coe, H., Ulbrich, I., Alfarra, M. R., Takami, A., Middlebrook, A. M., Sun, Y. L., Dzepina, K., Dunlea, E., Docherty, K, DeCarlo, P. F., Salcedo, D., Onasch, T., Jayne, J. T., Miyoshi, T., Shimono, A, Hatakeyama, S., Takegawa, N., Kondo, Y., Schneider, J., Drewnick, F., Borrmann, S, Weimer, S., Demerjian,

K., Williams, P., Bower, K., Bahreini, R., Cottrell, L., Griffin, R. J., Rautiainen, J., Sun, J. Y., and Zhang, Y. M.: Ubiquity and dominance of oxygenated species in organic aerosols in anthropogenically-influenced Northern Hemisphere midlatitudes, Geophy. Res. Lett., 34, L13801, 2007.

Zhang, Y., Xue, L., Carter, W. P. L., Pei, C., Chen, T., Mu, J., Wang, Y., Zhang, Q., and Wang, W.: Development of ozone reactivity scales for volatile organic compounds in a Chinese megacity, Atmos. Chem. Phys., 21, 11053-11068, 10.5194/acp-21-11053-2021, 2021.

Zhao, L., Li, P., and Yalkowsky, S. H.: Predicting the entropy of boiling for organic compounds, Journal of chemical information and computer sciences, 39, 1112-1116, 1999.

Zhou, C., Jang, M., and Yu, Z.: Simulation of SOA Formation from the Photooxidation of Monoalkylbenzenes in the Presence of Aqueous Aerosols Containing Electrolytes under Various NO_x Levels, Atmos. Chem. Phys., 19, 5719-5735, 2019.

Zuend, A., Marcolli, C., Booth, A. M., Lienhard, D. M., Soonsin, V., Krieger, U. K., Topping, D. O., McFiggans, G., Peter, T., and Seinfeld, J. H.: New and extended parameterization of the thermodynamic model AIOMFAC: calculation of activity coefficients for organic-inorganic mixtures containing carboxyl, hydroxyl, carbonyl, ether, ester, alkenyl, alkyl, and aromatic functional groups, Atmos. Chem. Phys., 11, 9155-9206, 10.5194/acp-11-9155-2011, 2011.

700 **Table 1.** Chamber experimental conditions for the SOA formation from the photooxidation of phenol and benzene under varying conditions.

HC	No.	Date	[a]Initial HC ppb	Initial NO$_x$ ppb	Initial HONO ppb	[b]HC/NOx ppbC/ppb	[c]Seed	Seed mass µg/m3	RH %	Temp K	[d]ΔHC µg/m3	[e]SOA Mass µg/m3	Yields	comments
Phenol	1	090721	79	85	N/A	5.6	No seed	N.A.	19-45	298-320	200	71	0.35	Fig. 4
	2	020723	227	104	N/A	13.1	No seed	N.A.	26-94	281-311	821	164	0.20	Fig. 3 Fig. 4
	3	090721	130	90	N/A	8.0	SA	332	15-56	296-320	185	48	0.25	Fig. 4
	4	020723	264	74	N/A	21.4	SA	129	25-89	281-308	546	164	0.30	Fig. 3 Fig. 4
	5	040623	92	59	N/A	9.4	AHS	2201	23-89	292-320	330	204	0.62	Fig. 3 Fig. 4
	6	040623	89	303	N/A	1.8	AHS	277	29-94	293-320	319	183	0.57	Fig. 4
	7	120222	148	54	N/A	16.4	d-AS	62	21-44	282-309	300	160	0.53	Fig. 3 Fig. 4
	8	120222	162	62	N/A	15.6	w-AS	141	59-98	282-309	319	179	0.56	Fig. 3 Fig. 4
Benzene	9	061722	292	32	75	16.4	No seed	N.A.	36-98	296-319	208	39.6	0.19	Fig. 3 Fig. 4
	10	061722	168	191	101	3.44	No seed	N.A.	24-84	296-322	163	13.5	0.08	Fig. 3
	11	080722	325	110	47	12.4	SA	372	21-56	297-319	112	29.4	0.26	Fig. 3 Fig. 4
	12	080722	310	303	74	4.9	SA	377	27-57	298-316	153	36.3	0.24	Fig. 4
	13	092022	266	65	77	11.2	AHS	95	27-93	295-320	134	32.9	0.25	Fig. 3 Fig. 4
	14	092022	233	341	71	3.39	AHS	153	38-99	295-318	112	20.4	0.18	Fig. 4
	15	121822	270	26	74	16.2	d-AS	10	27-54	281-301	125	42.6	0.34	Fig. 3 Fig. 4
	16	121822	238	21	61	17.4	w-AS	71	29-88	277-300	185	44.5	0.24	Fig. 3 Fig. 4

N.A.: not applicable

a. High NO$_x$: HC ppbC/NO$_x$ ppb < 5 ; low NO$_x$: HC/NO$_x$ > 5 ppbC/ppb

b. The seed condition refers to the injected electrolytic seed: sulfuric acid (SA), ammonium hydrogen sulfate (AHS), wet 705 ammonium sulfate (wet-AS), and dry AS (dry-AS).

c. ΔHC is difference between initial HC concentration and the HC concentration at 16:00 EST.

d. The SOA mass is determined with OC data at 16:00 EST.

e. The reported SOA mass was corrected for the particle loss to the chamber wall based on the 1st order deposition rate at 64 particle size beans. The dilution rate of SOA is estimated with the gas dilution factor determined using trace gas (CCl$_4$).

710
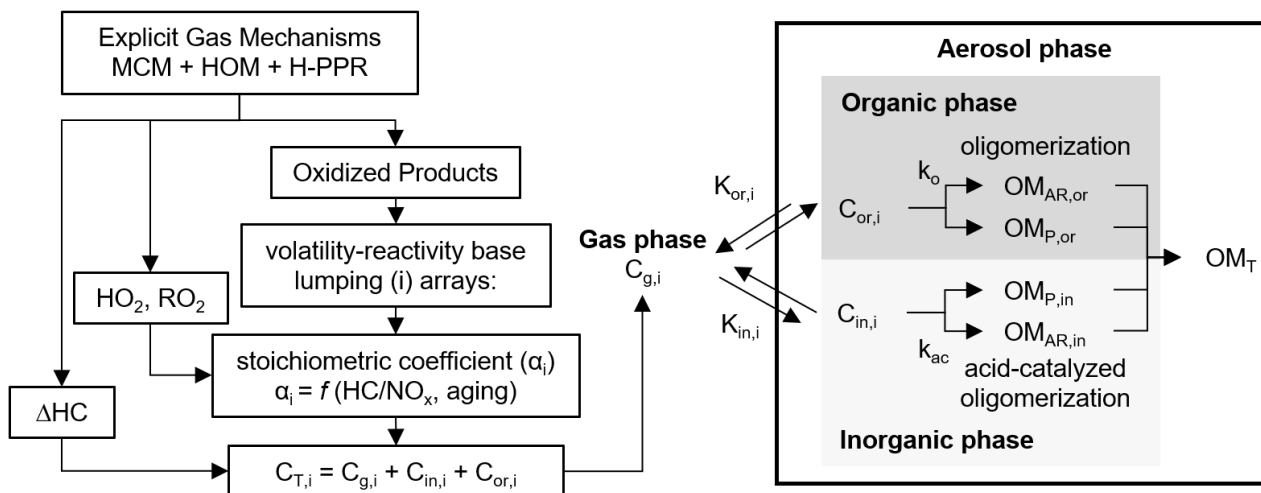
Figure 1: Scheme of the UNIPAR model to predict the SOA formation from the multiphase oxidation of phenol or benzene. The oxidized products predicted from the modified explicit gas mechanism (MCM v.3.3.1) integrated with the H-PPR model are classified into 50 lumping species (i) based on volatility and reactivity. The consumption of hydrocarbons (ΔHCs), the concentration of hydroperoxy radical (HO_2), alkylperoxy radical (RO_2), and the organic products are also simulated by using MCM and applied to the UNIPAR model. The lumping array associated with stoichiometric coefficients is dynamically constructed as a function of the HC ppbC/NOx ratio and the aging scale, which is estimated with the concentrations of HO_2 and RO_2 radicals. "C" denotes the concentration of an organic compound and K denotes partitioning coefficient of an organic compound. Subscripts "g", "or", and "in" represent gas, organic, and inorganic phases, respectively. OM refers the organic matter in aerosol. Subscripts "AR", "P", and "T" refer aerosol-phased reaction, partitioning, and total.
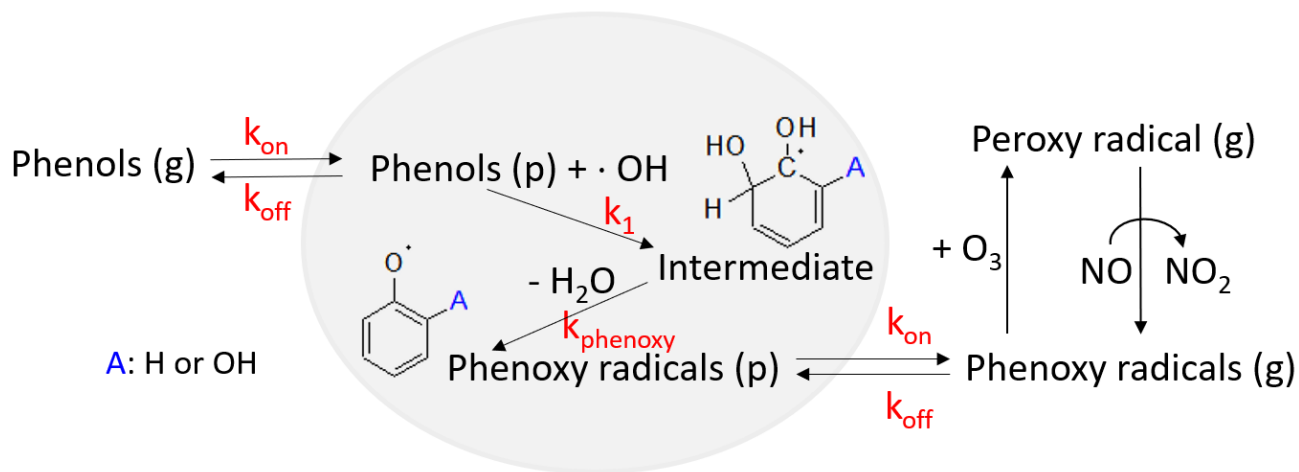
Figure 2 : The overview of the kinetic mechanisms, which streamlines the heterogeneous phenoxy radical formation (H-PPR) of gaseous phenols in the presence of acidic aerosol. k_{on} and k_{off} denote the uptake rate constant and the desorption rate constant, respectively for phenols in the presence of acidic aerosol. k_1 is the rate constant to heterogeneously form intermediates (hydroxy-phenols) and $k_{phenoxy}$ is the rate constant to from an intermediate to a phenoxy radical.
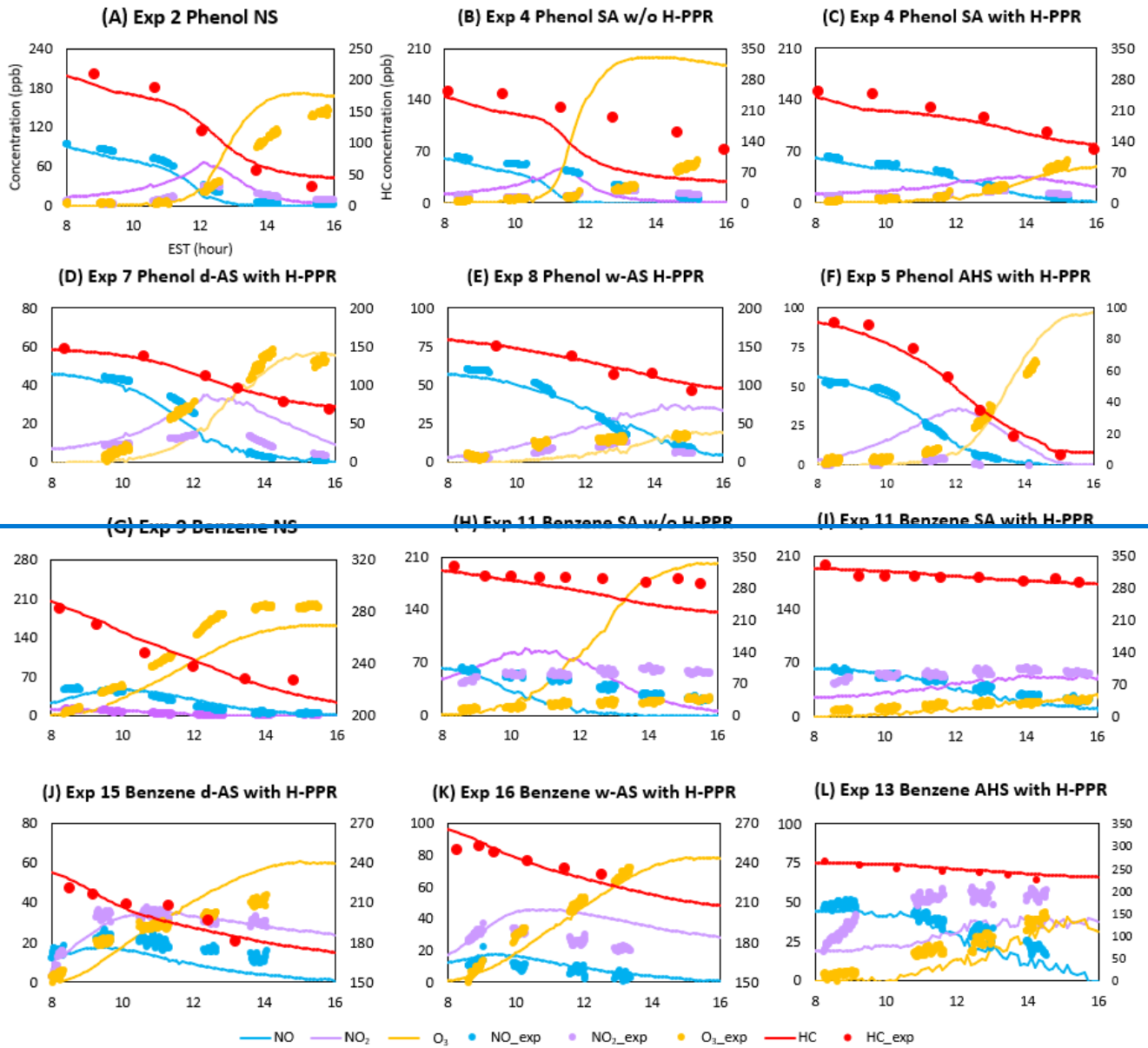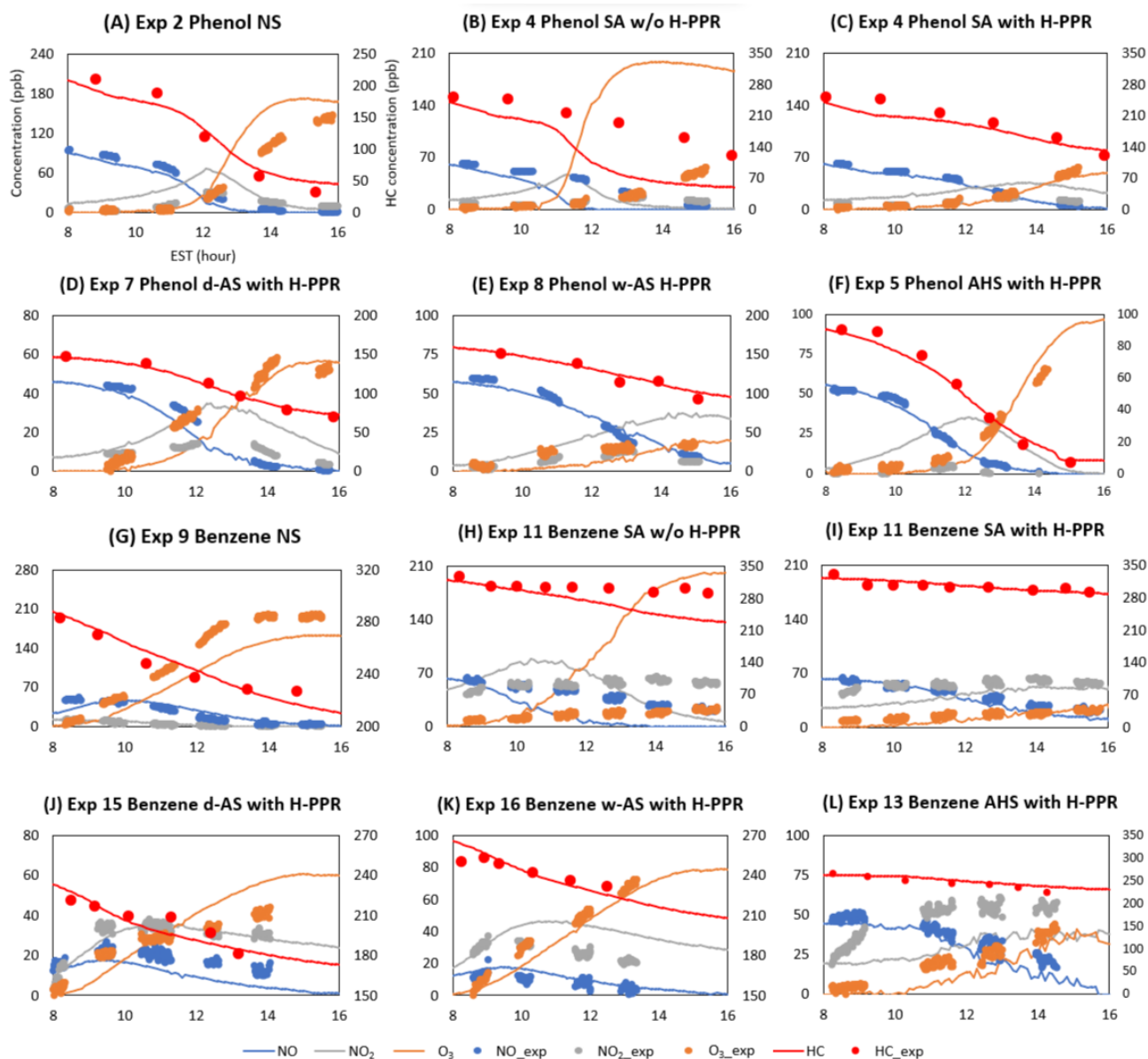
Figure 3 : The time profiles of observations and the prediction for concentrations of NO, NO₂, and O₃ and hydrocarbons (Table 1). The x-axis represents time (EST), the first y-axis represents the concentration (ppb) of gas species, and the second y-axis represents the hydrocarbon concentration in gas phase (ppb) as shown in (A). "HC" and "HC_exp" demote the gas simulation of hydrocarbons used in experiment and measurement of hydrocarbon used in experiment, respectively. The error associated with NO, NO₂, and O₃ are 2% and not visible in this Figure.
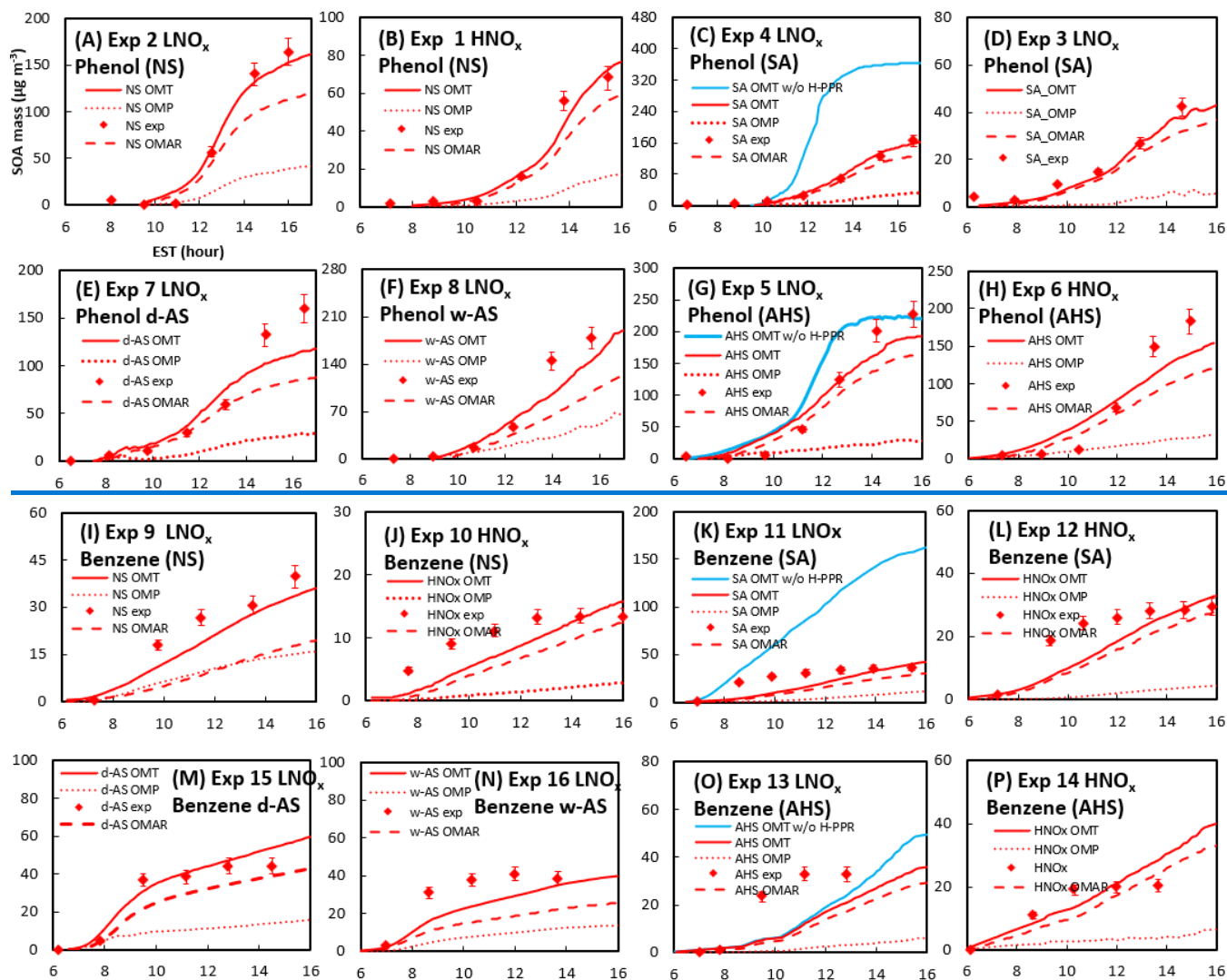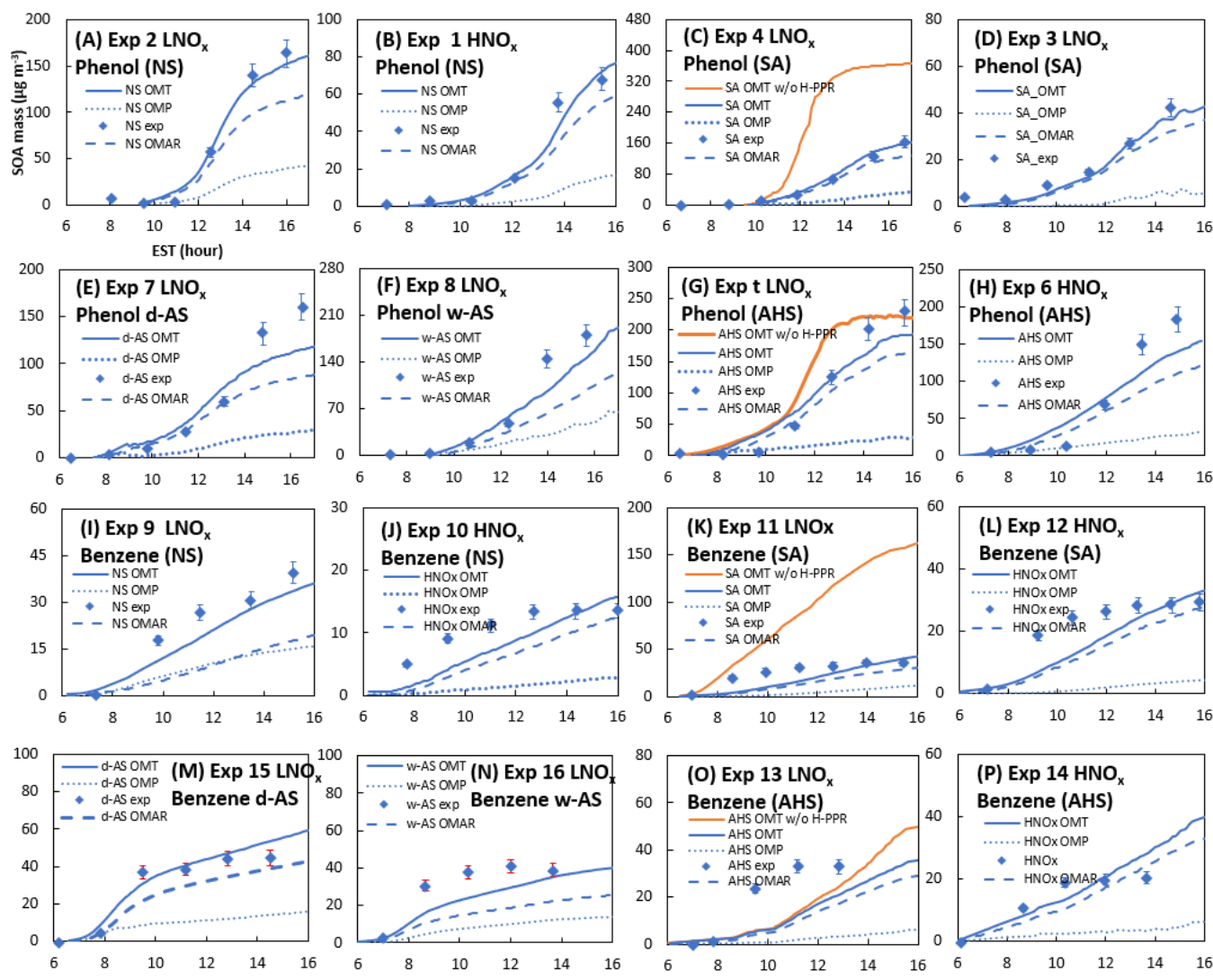
Figure 4 : The simulated SOA mass in the different seed condition and measured SOA mass in the different seed condition under different NO_x. Solid lines indicate the simulated SOA mass and bullet points (•) indicate the experimentally measured mass. The SOA mass simulated with the H-PPR model (red solid line) was compared with that simulated without the H-PPR model (blue solid line). The UNIPAR-predicted OM_{AR} (heterogeneous reaction in aerosol phase) and OM_p (partitioning) are also included. The error associated with SOA data was 9% according to the uncertainty in OC/EC data.
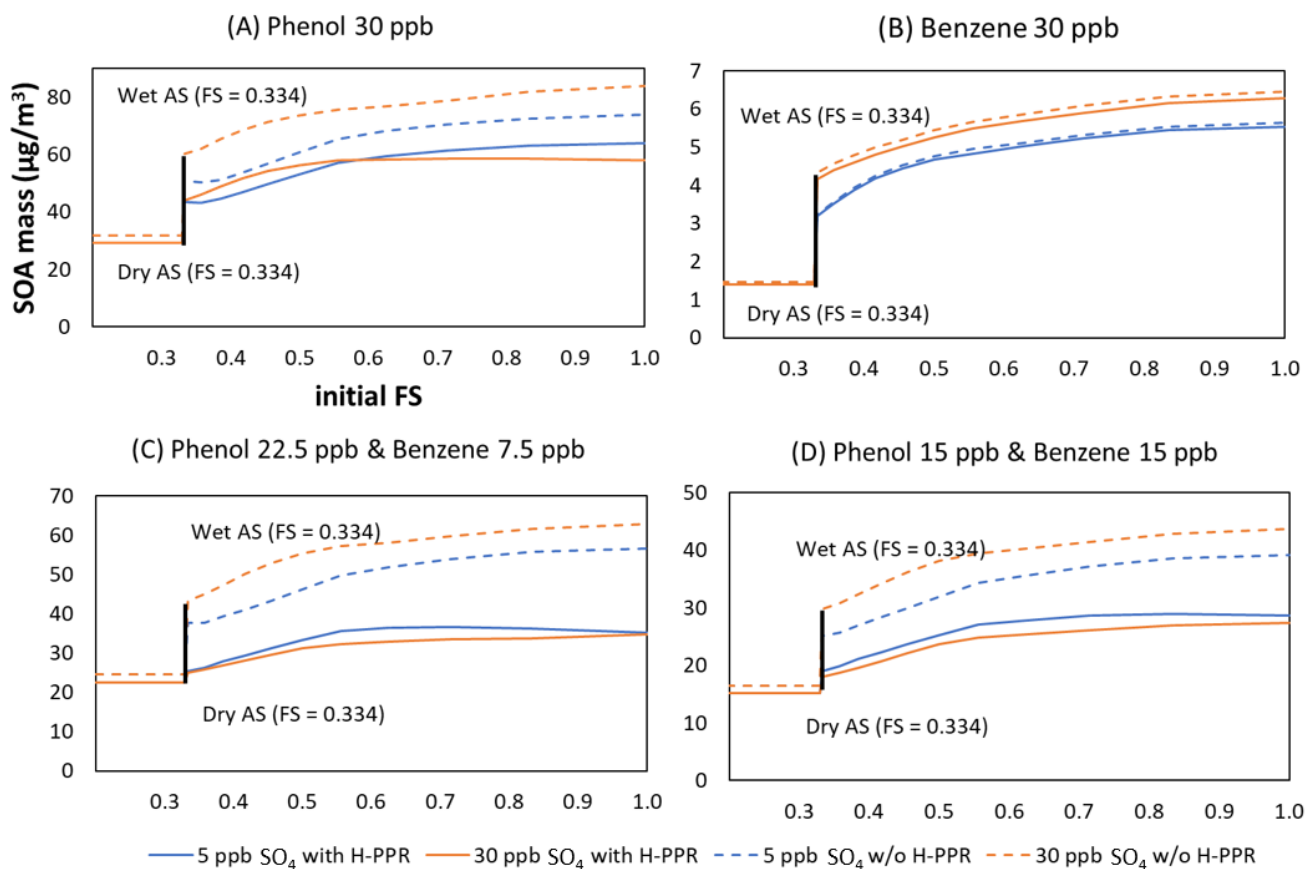
Figure 5. Sensitivity of SOA production to aerosol acidity (FS value) for different precursor mixes using the UNIPAR model: phenol (A), benzene (B), phenol:benzene = 3:1 ppb/ppb (C), and phenol:benzene = 1:1 ppb/ppb (D). The initial precursor hydrocarbon concentrations were 30 ppb. The initial concentrations of HONO, formaldehyde, acetaldehyde were 5 ppb, 6 ppb, and 2 ppb, respectively. The simulation was performed under ambient sunlight on October 19, 2022. RH was set to 0.6, temperature was to 298 K, and HC ppbC/NO_x ppb was 6. 5 ppb sulfate = 20 µg/m^3 and 30 ppb sulfate = 120 µg/m^3.
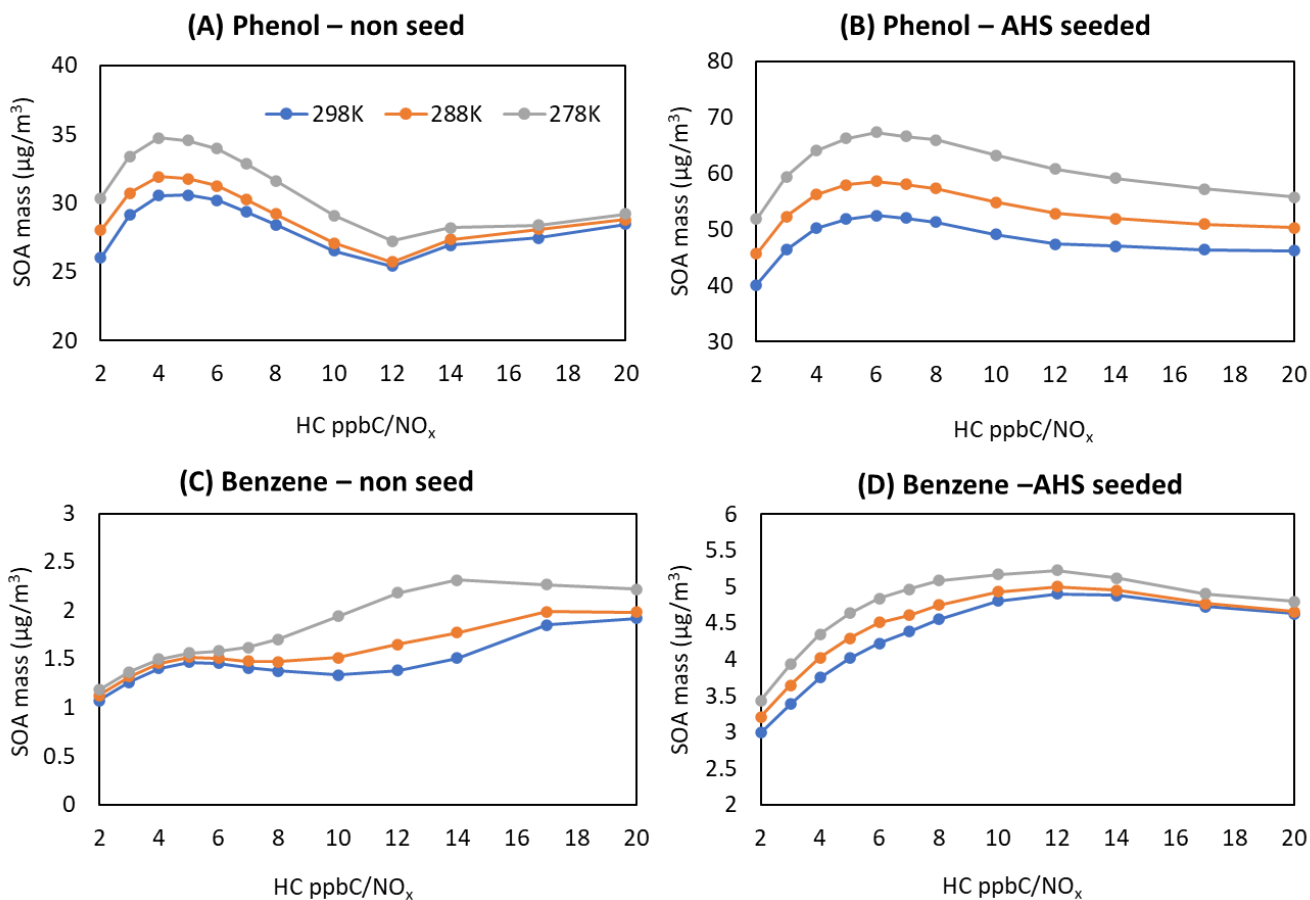
Figure 6. Sensitivity of SOA mass to major model variables. SOA simulations were performed at a given sunlight profile on October 19, 2022 (from 6:30 to 17:30, EST). All simulations were performed with 30 ppb of initial HC concentration. The predicted phenol SOA mass to NO_x levels three different temperature in the presence of ASH seed (A); the predicted phenol SOA mass to NO_x levels three different temperature in absence of seed (B); the predicted benzene SOA mass to NO_x levels three different temperature in the presence of ASH seed (C); and the predicted benzene SOA mass to NO_x levels three different temperature in absence of seed (D). Temperature levels were set to 298 K, 288 K, and 278 K. The NO_x levels (HC ppbC/NO_x ppb) range from 2 to 20.
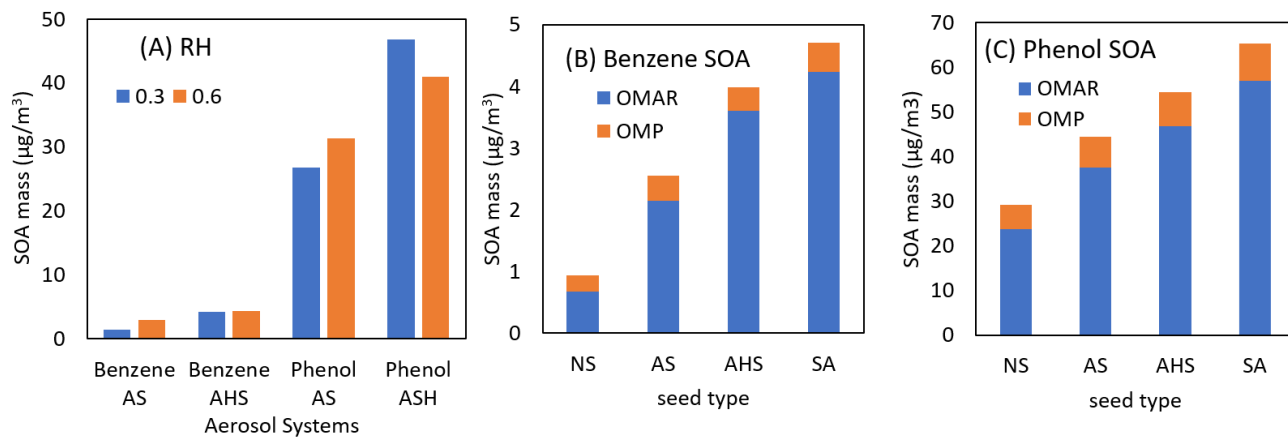
Figure 7. (A) The predicted SOA mass from the photooxidation of benzene or phenol at two different RH (0.3 and 0.6) in the presence of AS or AHS seed (HCpppbC/NO$_x$ = 6.64). OM$_{AR}$ (oligomeric mass) and OM$_P$ (partitioning mass) in benzene SOA (B) and phenol SOA (C). For (B) and (C), SOA production is simulated with initial HC concentration = 30 ppb (HC ppbC/NO$_x$ = 6.64), RH= 0.6, temperature = 298 K, and sulfate = 20 µg/m^3 under the sunlight condition on 10/19/2022.
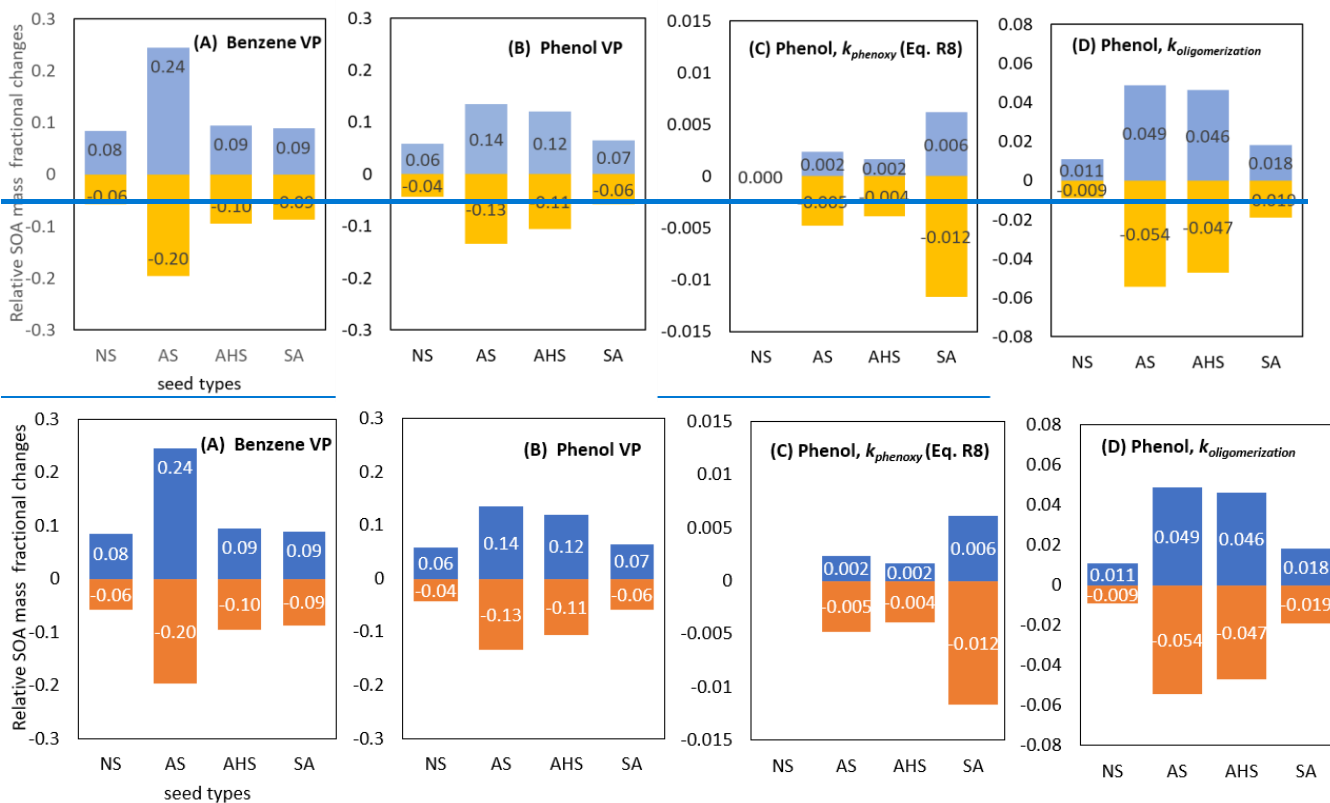
Figure 8. The relative change in SOA mass from the photooxidation of benzene or phenol. The variation in VP of benzene (A) and phenol (B), $k_{oligomerization}$ of phenol SOA (C) and $k_{phenoxy}$ of phenol SOA (D) is set to the factor of 0.5 and 2. SOA production is simulated with initial HC concentration = 30 ppb (HC ppbC/NO$_x$ = 6), RH= 0.6, temperature = 298 K, and sulfate = 20 µg/m^3 under the sunlight condition on 10/19/2022.